

# Choosing among notions of multivariate depth statistics

Karl Mosler

Institute of Econometrics and Statistics, University of Cologne

Pavlo Mozharovskyi

LTCI, Télécom Paris, Institut Polytechnique de Paris

April 3, 2020

## Abstract

Classical multivariate statistics measures the outlyingness of a point by its Mahalanobis distance from the mean, which is based on the mean and the covariance matrix of the data. A depth function is a function which, given a point and a distribution in  $d$ -space, measures centrality by a number between 0 and 1, while satisfying certain postulates regarding invariance, monotonicity, convexity and continuity. Accordingly, numerous notions of multivariate depth have been proposed in the literature, some of which are also robust against extremely outlying data. The departure from classical Mahalanobis distance does not come without cost. There is a trade-off between invariance, robustness and computational feasibility. In the last few years, efficient exact algorithms as well as approximate ones have been constructed and made available in R-packages. Consequently, in practical applications the choice of a depth statistic is no more restricted to one or two notions due to computational limits; rather often more notions are feasible, among which the researcher has to decide. We discuss the theoretical and practical aspects of this choice, including invariance and uniqueness, robustness and computational feasibility. Complexity and speed of exact algorithms are compared and the use of different depths in classification problems. The accuracy of approximate approaches like the random Tukey depth is discussed as well as the application to large and high-dimensional data. Also, local and functional depths are shortly addressed.

*AMS 2010 subject classifications:* Primary 62H05, 62H30; secondary 62-07.

*Keywords:* Depth statistics, DDalpha classification, computational complexity, robustness, approximation, random Tukey depth.

# 1 Introduction

Many statistical tasks involve measures of centrality, identifying the center of a data cloud and measuring how close a given data point is to the center. In a probabilistic setting, we are interested in the question how central a point lies in a probability distribution. The opposite of centrality is outlyingness. Classical multivariate statistics measures outlyingness by the Mahalanobis distance. This is the usual Euclidean distance applied to ‘sphered’ or ‘whitened’ data, being transformed by a center point and a scatter matrix. Since the early 1990’s more general statistics have been developed for measuring centrality and outlyingness of data in  $\mathbb{R}^d$  as well as for identifying central regions of a data cloud, consisting of points having at least a given centrality. Though depth originates from data analysis and has been principally introduced for empirical distributions, most notions of depth allow for a *population version*, that is, can be defined for general probability distributions beyond empirical ones.

In general, a ( $d$ -variate) *depth function* is a function  $D : (\mathbf{y}, P) \mapsto [0, 1]$ , for  $\mathbf{y} \in \mathbb{R}^d$  and  $P$  from some class  $\mathcal{P}$  of  $d$ -variate probability distributions, that satisfies several postulates regarding invariance, monotonicity, convexity and continuity. We write  $D(\mathbf{y}|\mathbf{X})$  in place of  $D(\mathbf{y}|P)$ , where  $\mathbf{X}$  denotes a random variable distributed as  $P$ . An often-quoted set of such postulates has been given in Zuo and Serfling (2000). Here we use a slightly terser one, which is due to Dyckerhoff (2002):  $D$  is a depth function if it is invariant against  $\mathbb{R}^d$ -transformations in some class  $\mathcal{T}$ , null at infinity, monotone decreasing on rays from its maximum, and upper continuous. Formally, for  $\mathbf{y} \in \mathbb{R}^d$  and  $P \in \mathcal{P}$ ,

- **$\mathcal{T}$ -Invariance:**  $D(T(\mathbf{y})|T(\mathbf{X})) = D(\mathbf{y}|\mathbf{X})$  for all  $T \in \mathcal{T}$ ,
- **Null at infinity:**  $\lim_{\|\mathbf{y}\| \rightarrow \infty} D(\mathbf{y}|\mathbf{X}) = 0$ .
- **Monotone on rays:** If a point  $\mathbf{y}^*$  has maximal depth, that is  $D(\mathbf{y}^*|\mathbf{X}) = \max_{\mathbf{y} \in \mathbb{R}^d} D(\mathbf{y}|\mathbf{X})$  then for any  $\mathbf{r}$  in the unit sphere of  $\mathbb{R}^d$  the function  $\gamma \mapsto D(\mathbf{y}^* + \gamma\mathbf{r}|\mathbf{X})$  does not increase with  $\gamma > 0$ .
- **Upper semicontinuous:** The upper level sets  $D^\alpha = \{\mathbf{z} \in \mathbb{R}^d | D(\mathbf{z}|\mathbf{X}) \geq \alpha\}$  are closed for all  $\alpha \in [0, 1]$ .

Any point  $\mathbf{y}^*$  that has maximum depth is called a *median*. The postulates imply that the level sets (= *central regions*)  $D^\alpha$ ,  $\alpha \in ]0, 1]$ , are bounded and starshaped about  $\mathbf{y}^*$ . Moreover, if  $\mathbf{X}$  is centrally symmetric about some  $\mathbf{z}^* \in \mathbb{R}^d$ , then any depth function yields  $\mathbf{z}^*$  as a median. Recall that  $\mathbf{X}$  is *centrally symmetric* about  $\mathbf{z}^*$  if  $\mathbf{X} - \mathbf{z}^*$  has the same distributions as  $\mathbf{z}^* - \mathbf{X}$ . If the level sets are convex,  $D$  is a *quasi-convex depth function*. Mostly,  $\mathcal{T}$  is specified as the class of affine transformations of  $\mathbb{R}^d$ , but other classes of transformations are possible and of practical interest.

Central regions are sometimes parameterized by their probability content,

$$D_\beta(\mathbf{X}) = \bigcap_{\alpha \in A(\beta)} D^\alpha(\mathbf{X}), \quad \text{where} \quad A(\beta) = \{\alpha : P[D^\alpha(\mathbf{X})] \geq \beta\}. \quad (1)$$

If  $P$  is the empirical distribution on a set  $\{\mathbf{x}_1, \dots, \mathbf{x}_n\}$  of data points, the depth function is mentioned as a *multivariate data depth* and written  $D(\mathbf{y}|\mathbf{x}_1, \dots, \mathbf{x}_n)$ .

Well-known examples of depth functions are the *halfspace depth* (Tukey, 1975), which is also called *Tukey* or *location depth*, the *zonoid depth* (Koshevoy and Mosler, 1997), the *spatial* (Serfling, 2002), *projection* (Liu, 1992; Zuo and Serfling, 2000), *simplicial* (Liu, 1990) and *simplicial volume* (Oja, 1983) *depths*. A more recent notion is the  $\beta$ -*skeleton depth* (Yang and Modarres, 2018), which includes the *lens depth* (Liu and Modarres, 2011) and the *spherical depth* (Elmore et al., 2006) as special cases; see Section 2 below. These depth functions differ in their analytical properties and computational feasibility. When it comes to applications the problem arises which of these depth notions should be employed in a given situation.

Depth statistics have been used in numerous and diverse tasks of which we can mention a few only. Liu et al. (1999) provide an introduction to some of them. Given data in  $\mathbb{R}^d$ , central regions are *set-valued statistics*. They are used to describe and compare multivariate distributions w.r.t. location, dispersion, and shape, to identify outliers of a distribution (Chen et al., 2009), to classify and cluster data (Hoberg, 2000; Lange et al., 2014b), to test for multivariate scale and symmetry (Dyckerhoff, 2002; Dyckerhoff et al., 2015). Also, to measure multidimensional risk (Cascos and Molchanov, 2007), and to handle constraints in stochastic optimization (Mosler and Bazovkin, 2014), among others.

Actually, a plethora of depth notions can be defined that satisfy the postulates, and too many different notions have already been proposed in the literature. Classical multivariate statistics based on Mahalanobis distance always yields elliptical central regions, which correspond to a model assumption of elliptically symmetric probability distributions. In contrast, other depth statistics adapt better to non-symmetric distributions. Some depth statistics are also robust against possibly contaminated data. The departure from classical Mahalanobis distance does not come without cost. The computational load cannot be neglected, gaining weight with the number  $n$  of data and, even more, with dimension  $d$ . Therefore, until recently, due to computational infeasibility the use of most depth statistics was limited to small  $n$  and  $d$  in applications, and the choice of a proper depth statistic in practice was restricted to very few notions.

But in the last few years, efficient algorithms have been constructed. Procedures for many notions of multivariate and functional data depth have been made available in R-packages and applied to various tasks; see Pokotylo et al. (2019) for `ddalpha`, Genest et al. (2017) for `depth`, Hubert et al. (2015) for `mrf.Depth`, Kosiorowski and Zawadzki (2014)

for `DepthProc`, and Febrero-Bande and de la Fuente (2012) for `fda.usc`. For details see Section 5.3 below.

These packages allow, together with the secular increase in computing power, the numerical treatment of depth statistics in applications having realistic sizes of  $n$  and  $d$ . Consequently, the choice of a depth statistic is not any more restricted to one or two notions due to computational limits, but rather often to more notions of depth among which we have to decide.

Also, depth notions for functional data have raised considerable interest in the recent literature. Most of them build on depths for finite dimensional data, so that their properties (including computability) depend on that of the multivariate depths involved.

In this paper we discuss aspects and general principles that guide us in this choice. They are useful in the construction of depth-based statistical procedures as well as in practical applications when several notions of depth appear to be computationally feasible.

In Section 2 we review eleven depth statistics. Section 3 discusses their analytical properties: invariance, depth-trimmed regions, uniqueness of the underlying distribution, and continuity. Section 4 is about possible specifics of the data, such as symmetry of the generating law and the existence of outliers. It includes a comparative study of depth-based classification under different distributions of data. Section 5 treats the computational feasibility of the depth notions; times for their exact computation are compared, approximate procedures discussed, and the approximation error of the random Tukey depth (Cuesta-Albertos and Nieto-Reyes, 2008a) is calculated. Existing implementations of exact and approximate procedures are shortly surveyed. Then, dealing with large and high-dimensioned data is discussed. Section 6 addresses extensions to local and functional depths. Section 7 concludes with practical guidelines. More results are found in the Supplementary Material.

## 2 Some popular depth statistics

Many depth notions have been proposed in the literature. Not all of them satisfy the above postulates. We review several most relevant ones in terms of analytical and computational feasibility and in view of applied work. (For some of them,  $\mathbf{X}$  has to satisfy moment conditions or other obvious restrictions.)

- **Mahalanobis depth** (Mahalanobis, 1936):

$$D_{Mah}(\mathbf{y}|\mathbf{X}) = (1 + \|\mathbf{y} - \boldsymbol{\mu}_{\mathbf{X}}\|_{\Sigma_{\mathbf{X}}}^2)^{-1} \quad (2)$$

is called (*moment*) *Mahalanobis depth*. Here,  $\boldsymbol{\mu}_{\mathbf{X}}$  and  $\Sigma_{\mathbf{X}}$  denote the expectation vector and the covariance matrix of  $\mathbf{X}$ , and  $\|\mathbf{z}\|_{\Sigma_{\mathbf{X}}}^2 = \mathbf{z}^T \Sigma_{\mathbf{X}}^{-1} \mathbf{z}$  is the *Mahalanobis norm* of  $\mathbf{z} \in \mathbb{R}^d$ .

- **$\mathbb{L}_p$  depth** (Zuo and Serfling (2000)):

$$D_{\mathbb{L}_p}(\mathbf{y}|P) = (1 + E\|\mathbf{y} - \mathbf{X}\|_p)^{-1}, \quad (3)$$

$1 \leq p < \infty$ . The depth  $D_{\mathbb{L}_p}$  is based on the expected outlyingness of a point, as measured by the  $\mathbb{L}_p$ -distance. For  $p = 2$  it is also mentioned as *Euclidean depth*.

- **Halfspace depth ( = location depth = Tukey depth)** (Tukey, 1975; Donoho and Gasko, 1992):

$$D_H(\mathbf{y}|\mathbf{X}) = \inf\{Pr[\mathbf{X} \in H] : H \text{ closed halfspace, } \mathbf{y} \in H\}. \quad (4)$$

- **Projection depth** (Liu, 1992; Zuo and Serfling, 2000):

$$D_{Proj}(\mathbf{y}|\mathbf{X}) = \left(1 + \sup_{\mathbf{p} \in S^{d-1}} \frac{|\langle \mathbf{p}, \mathbf{y} \rangle - \text{med}(\langle \mathbf{p}, \mathbf{X} \rangle)|}{\text{MAD}(\langle \mathbf{p}, \mathbf{X} \rangle)}\right)^{-1}, \quad (5)$$

where  $\text{med}(V)$  denotes the median of a univariate random variable  $V$ , and  $\text{MAD}(V) = \text{med}(|V - \text{med}(V)|)$  its median absolute deviation from the median.

- **Simplicial depth** (Liu, 1990):

$$D_{Sim}(\mathbf{y}|\mathbf{X}) = Pr[\mathbf{y} \in \text{conv}(\{\mathbf{X}_1, \dots, \mathbf{X}_{d+1}\})], \quad (6)$$

where  $\mathbf{X}_1, \dots, \mathbf{X}_{d+1}$  are i.i.d. copies of  $\mathbf{X}$ , and  $\text{conv}$  means convex hull.

- **Simplicial volume depth ( = Oja depth)** (Oja, 1983; Zuo and Serfling, 2000): For any points  $\mathbf{v}_1, \dots, \mathbf{v}_{d+1} \in \mathbb{R}^d$ , the convex hull  $\text{conv}(\{\mathbf{v}_1, \dots, \mathbf{v}_{d+1}\})$  has  $d$ -dimensional volume

$$\text{vol}_d(\text{conv}\{\mathbf{v}_1, \dots, \mathbf{v}_{d+1}\}) = \frac{1}{d!} |\det((1, \mathbf{v}_1^\top)^\top, \dots, (1, \mathbf{v}_{d+1}^\top)^\top)|.$$

The *simplicial volume depth* or *Oja depth* is defined by

$$D_{Oja}(\mathbf{y}|\mathbf{X}) = (1 + E[\text{vol}_d(\text{conv}\{\mathbf{y}, \mathbf{X}_1, \dots, \mathbf{X}_d\})])^{-1}, \quad (7)$$

where  $\mathbf{X}_1, \dots, \mathbf{X}_d$  are independent copies of  $\mathbf{X}$ .

- **Zonoid depth** (Koshevoy and Mosler, 1997): For  $0 < \alpha \leq 1$ ,

$$D_{Zon}^\alpha(\mathbf{X}) = \left\{ E[\mathbf{X} g(\mathbf{X})] : g : \mathbb{R}^d \rightarrow [0, 1/\alpha] \text{ measurable and } E[g(\mathbf{X})] = 1 \right\} \quad (8)$$

is the *zonoid  $\alpha$ -region* of  $\mathbf{X}$ . For  $\alpha = 0$  set  $D_{Zon}^0(\mathbf{X}) = \mathbb{R}^d$ . The *zonoid depth* is defined as

$$D_{Zon}(\mathbf{y}|\mathbf{X}) = \sup\{\alpha : \mathbf{y} \in D_{Zon}^\alpha(\mathbf{X})\} \quad (9)$$

For an empirically distributed  $\mathbf{X}$  the zonoid depth then is calculated as

$$D_{Zon}(\mathbf{y}|\mathbf{X}) = \sup \left\{ \alpha : \alpha \lambda_i \leq 1/n, \mathbf{y} = \sum_{i=1}^n \lambda_i \mathbf{x}_i, \sum_{i=1}^n \lambda_i = 1, \lambda_i \geq 0 \ \forall i \right\}. \quad (10)$$

- **Spatial depth** (Serfling, 2002): The *spatial depth* is defined as

$$D_{Spa}(\mathbf{y}|\mathbf{X}) = 1 - \left\| E \frac{\mathbf{y} - \mathbf{X}}{\|\mathbf{y} - \mathbf{X}\|} \right\|, \quad (11)$$

where we set  $0/0 = 0$ .

- **Lens depth** (Liu and Modarres, 2011): A function  $v : \mathbb{R}^d \times \mathbb{R}^d \rightarrow \mathbb{R}_+$  is a *dissimilarity function* if it is symmetric,  $v(\mathbf{x}, \mathbf{y}) = v(\mathbf{y}, \mathbf{x})$ , and vanishes if and only if  $\mathbf{x}$  and  $\mathbf{y}$  are the same,  $v(\mathbf{x}, \mathbf{y}) = 0 \Leftrightarrow \mathbf{x} = \mathbf{y}$ . Note that every distance is a dissimilarity function. Assume that for any three values  $\mathbf{x}, \mathbf{y}, \mathbf{z}$  of a random vector  $\mathbf{X}$  in  $\mathbb{R}^d$  the following information is given: One of these points, say  $\mathbf{x}$ , is more similar (= less dissimilar) to each of the two other points than these are among themselves, i.e.

$$v(\mathbf{x}, \mathbf{y}) < v(\mathbf{y}, \mathbf{z}) \quad \text{and} \quad v(\mathbf{x}, \mathbf{z}) < v(\mathbf{y}, \mathbf{z}), \quad (12)$$

in symbols  $\mathbf{x} \triangleleft (\mathbf{y}, \mathbf{z})$ . It means that  $\mathbf{x}$  is the “most central” among the three points. This information will be mentioned as *ordinal dissimilarity information* on  $\mathbf{X}$ .

Given such ordinal dissimilarity information, the *lens depth* can be defined as follows (Kleindessner and Von Luxburg, 2017):

$$D_{Lens}(\mathbf{y}|\mathbf{X}) = Pr[\mathbf{y} \triangleleft (\mathbf{X}_1, \mathbf{X}_2)], \quad (13)$$

where  $\mathbf{X}_1$  and  $\mathbf{X}_2$  are independent copies of  $\mathbf{X}$ . If dissimilarity is measured by the Euclidean distance we get:

$$D_{Lens}^{Eucl}(\mathbf{y}|\mathbf{X}) = Pr[\max\{\|\mathbf{y} - \mathbf{X}_1\|, \|\mathbf{y} - \mathbf{X}_2\|\} < \|\mathbf{X}_1 - \mathbf{X}_2\|] \quad (14)$$

- **$\beta$ -skeleton depths** (Yang and Modarres, 2018): Depending on a parameter  $\beta \geq 1$  Yang and Modarres (2018) introduced the  *$\beta$ -skeleton depths*,

$$D_{Skel\beta}(\mathbf{y}|\mathbf{X}) = Pr[\|\mathbf{y} - \mathbf{X}_{1\beta 2}\| < \beta/2 \|\mathbf{X}_1 - \mathbf{X}_2\| \text{ and } \|\mathbf{y} - \mathbf{X}_{2\beta 1}\| < \beta/2 \|\mathbf{X}_1 - \mathbf{X}_2\|], \quad (15)$$

where  $\mathbf{X}_{1\beta 2} = \beta/2 \mathbf{X}_1 + (1 - \beta/2) \mathbf{X}_2$ . With  $\beta = 2$  the *Euclidean lens depth* (14) is obtained, and with  $\beta = 1$  the so called *spherical depth* (Elmore et al., 2006),

$$D_{Sph}(\mathbf{y}|\mathbf{X}) = Pr[\|\mathbf{y} - (\mathbf{X}_1 + \mathbf{X}_2)/2\| < \|\mathbf{X}_1 - \mathbf{X}_2\|/2]. \quad (16)$$

- **Convex hull peeling depth ( = onion depth)** (Barnett, 1976; Eddy, 1981): The convex hull peeling depth is defined only for an empirical distribution of  $\mathbf{X}$ , say on the finite set  $S_{\mathbf{X}}$ . Consider the sequence of closed convex sets (= *onion layers*)

$$C_1(\mathbf{X}) = \text{conv}(S_{\mathbf{X}}), \quad C_{j+1}(\mathbf{X}) = \text{conv}(S_{\mathbf{X}} \cap \text{int } C_j(\mathbf{X})), \quad j = 1, 2, \dots \quad (17)$$

Here  $\text{int}$  denotes the interior of a set. Define the *convex hull peeling* (or *onion*) *depth* of  $\mathbf{y}$  as the smallest index  $j$  at which  $\mathbf{y} \in C_j$ , i.e.

$$D_{CHP}(\mathbf{y}|\mathbf{X}) = \sum_{j \geq 1} \mathbf{1}_{\text{int } C_j(\mathbf{X})}(\mathbf{y}), \quad (18)$$

with  $\mathbf{1}_S$  denoting the indicator function of a set  $S$ .

Figure 1 exhibits, for nine notions of depth, central regions of bivariate macroeconomic data (unemployment and public debt in 2018) of all 28 countries of the European Union. For lens depth see Figure 2.

### 3 Relevant properties

As we see from Figure 1, different depths yield different central regions. Consequently, when these depths are employed, e.g. to find outliers or to classify data, different results will arise. Therefore we have to distinguish the specific aspects of the various depths. In the sequel we discuss properties of the depth notions. (Note that for reasons of practicality and comparison these properties are not always given in their most general form.) Many properties of Mahalanobis,  $\mathbb{L}_p$ -, halfspace, simplicial, projection, and Oja depth are demonstrated in Zuo and Serfling (2000). Particularly, see Donoho and Gasko (1992) for halfspace depth, Zuo and Serfling (2000) for  $\mathbb{L}_p$ -depth, Serfling (2002) for spatial depth, Mosler (2002) for zonoid depth, Zuo et al. (2003) for projection depth. For  $\beta$ -skeleton and lens depth refer to Liu and Modarres (2011) and Yang and Modarres (2018), and for onion depth to Donoho and Gasko (1992) and Liu et al. (1999).

#### 3.1 Invariance of depth statistic

A principal aspect of any statistical procedure is invariance: Which features of the data shall the statistic ignore, and which shall it reflect?

Table 1 specifies relevant classes  $\mathcal{T}$  of transformations of  $\mathbb{R}^d$  to which a depth function  $D$  may be invariant,  $D(T(\mathbf{y})|T(\mathbf{X})) = D(\mathbf{y}|\mathbf{X})$  for all  $T \in \mathcal{T}$ .

A depth is *combinatorially invariant* if it is invariant against combinatorially equivalent transformations of its arguments  $\mathbf{y}, \mathbf{x}_1, \dots, \mathbf{x}_n$ . A transformation of data is mentioned as *combinatorially equivalent* if, besides renumbering, none of the data crosses a hyperplane

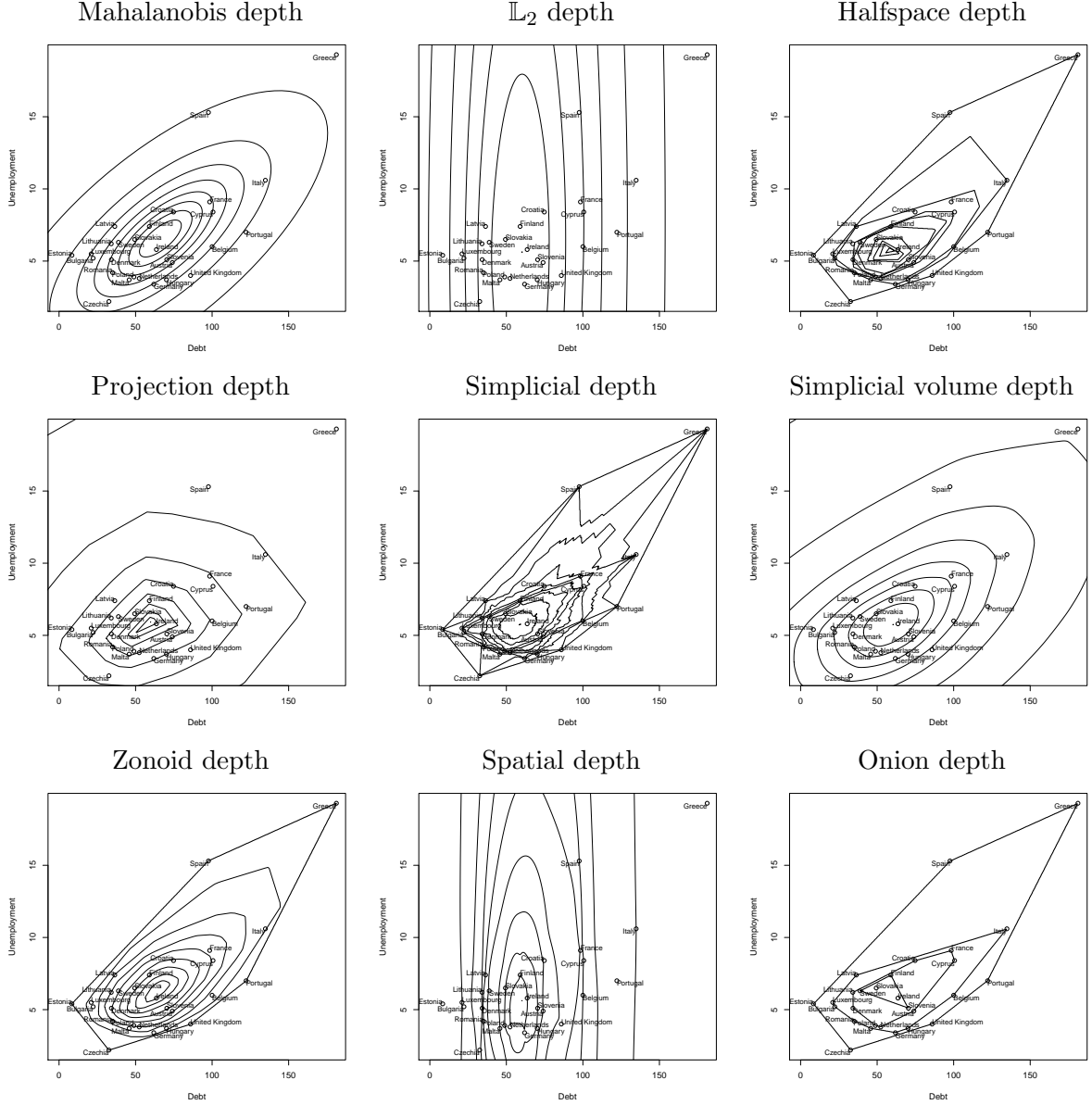


Figure 1: Central regions of EU data on unemployment and public debt in 2018 (Source: EUROSTAT), for nine notions of depth.



| $\mathcal{T}$       | Name                    | Transformation   |   |
|---------------------|-------------------------|--|---|
| $\mathcal{T}_A$     | affine                  | $\mathbf{x} \mapsto \mathbf{A}\mathbf{x} + \mathbf{b}$ | $\mathbf{A} \in \mathbb{R}^{d \times d}$ regular, $\mathbf{b} \in \mathbb{R}^d$ |
| $\mathcal{T}_O$     | orthogonal              | $\mathbf{x} \mapsto \mathbf{A}\mathbf{x}$              | $\mathbf{A} \in \mathbb{R}^{d \times d}$ , $\mathbf{A}\mathbf{A}^T = I_d$       |
| $\mathcal{T}_T$     | translation             | $\mathbf{x} \mapsto \mathbf{x} + \mathbf{b}$           | $\mathbf{b} \in \mathbb{R}^d$   |
| $\mathcal{T}_{cSc}$ | coordinate-wise scaling | $\mathbf{x} \mapsto \mathbf{\Lambda}\mathbf{x}$        | $\mathbf{\Lambda} = \text{diag}(\lambda_1, \dots, \lambda_d)$ , $\lambda_j > 0$ |
| $\mathcal{T}_{uSc}$ | uniform scaling         | $\mathbf{x} \mapsto \lambda\mathbf{x}$                 | $\lambda > 0$   |
| $\mathcal{T}_{Com}$ | combinatorial           | $T$ combinatorial transformation                       |   |
| $\mathcal{T}_{OD}$  | ordinal dissimilarity   | $T$ stretching transformation                          |   |

Table 1: Classes of transformations for invariance of depth functions.

spanned by  $d$  other data points; more precisely, if the set of minimal Radon partitions of the data remains unchanged (see Section 4.4. in Mosler (2002)). Then, in particular, any point that lies on the convex hull border of the data can be moved far away from the data cloud without changing its depth. Consequently, a combinatorially invariant depth is very robust against outlying data, while it is *not* useful in identifying outliers. Note that combinatorial invariance is defined on empirical distributions only. A depth that is combinatorially invariant is named a *combinatorial depth*.

Halfspace depth, simplicial depth, and onion depth are combinatorially invariant; see e.g. Cor. 4.12 in Mosler (2002). In contrast, other depths are not combinatorially invariant, as they use distances in  $\mathbb{R}^d$ : Mahalanobis,  $\mathbb{L}_2$  depth, projection, and simplicial volume depth. Also the zonoid depth as well as the weighted-mean depths (Dyckerhoff and Mosler, 2011) use the metrical structure of  $\mathbb{R}^d$ .

By a *stretching transformation* we mean a transformation of the data that leaves the ordinal dissimilarity information unchanged. E.g., the lens depth with general (ordinal only) dissimilarity function is *ordinal dissimilarity invariant*. Note that, if the information is metrical and  $v$  is the Euclidean (resp. Mahalanobis) distance, then the lens depth is orthogonal and translation (resp. affine) invariant.

Many multivariate depths are *affine invariant*, which is often considered as a standard requirement. These depths are independent of any specific coordinate system in  $\mathbb{R}^d$ . Examples are the Mahalanobis, halfspace, projection, simplicial, zonoid, and onion depths. Affine invariance may hold only up to a positive scalar factor; this is mentioned as *weak affine invariance*.

Some depths are basically invariant only to orthogonal transformations, translations and uniform scaling, among them the Euclidean, spatial, simplicial volume, and  $\beta$ -skeleton depths. These depths can be made affine invariant by a scatter matrix transform.

A *scatter matrix*  $\mathbf{R}_\mathbf{X}$  (also called *scatter functional*) is a symmetric positive definite  $d \times d$  matrix that depends continuously (in weak convergence) on the distribution of  $\mathbf{X}$

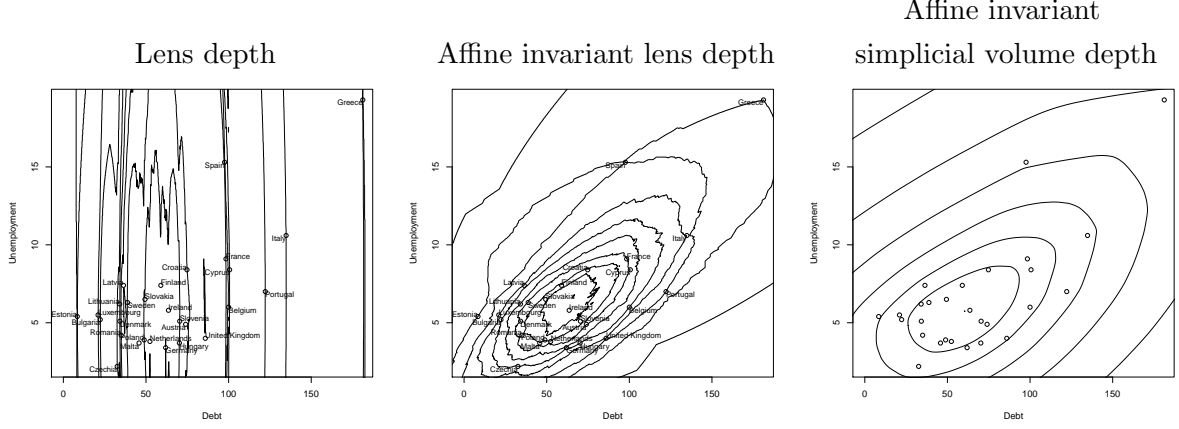


Figure 2: Central regions of EU data on unemployment and public debt in 2018 (Source: EUROSTAT): lens depth, affine invariant lens depth, and affine invariant simplicial volume depth ( $\mathbf{R}$  = covariance matrix).

and measures its spread in an affine equivariant way. The latter means that

$$\mathbf{R}_{\mathbf{A}\mathbf{X}+\mathbf{b}} = \lambda_{\mathbf{X},\mathbf{A},\mathbf{b}} \mathbf{A} \mathbf{R}_{\mathbf{X}} \mathbf{A}^T \quad \text{holds for any } \mathbf{A} \text{ of full rank and any } \mathbf{b}, \quad (19)$$

with some  $\lambda_{\mathbf{X},\mathbf{A},\mathbf{b}} > 0$ . The data is transformed as

$$\mathbf{x} \mapsto \mathbf{R}_{\mathbf{X}}^{-1/2}(\mathbf{x} - \theta(\mathbf{X})), \quad (20)$$

where  $\mathbf{R}_{\mathbf{X}}$  is a scatter matrix and  $\theta(\mathbf{X})$  a location parameter. This scatter matrix transformation is also mentioned as *sphering* or *whitening* the data.

E.g., the simplicial volume depth (7) is only orthogonal invariant. Its affine invariant version is given by

$$D_{Oja}^*(\mathbf{y}|\mathbf{X}) = \left( 1 + \frac{E[\text{vol}_d(\text{conv}\{\mathbf{y}, \mathbf{X}_1, \dots, \mathbf{X}_d\})]}{\sqrt{\det \mathbf{R}_{\mathbf{X}}}} \right)^{-1}, \quad (21)$$

Similarly, the lens depth (13) is made affine invariant. Central regions of lens depth, affine invariant lens depth, and affine invariant simplicial volume depth are shown in Figure 2.

Clearly, there are many ways to choose a matrix that satisfies (19). A most prominent example for  $\mathbf{R}_{\mathbf{X}}$  is the covariance matrix  $\Sigma_{\mathbf{X}}$  of  $\mathbf{X}$ . (Observe that the covariance matrix is positive definite, if the convex hull of the support of  $\mathbf{X}$  has full dimension.) If robustness is an issue, proper choices for the scatter matrix  $\mathbf{R}_{\mathbf{X}}$  are the *minimum volume ellipsoid* (MVE) estimator, the *minimum covariance determinant* (MCD) estimator and similar robust covariance estimators; see Rousseeuw and Leroy (1987) and Lopuhaa et al. (1991) and Section 4.2 below.

However, many classical multivariate procedures are less than affine invariant and, if combined with a depth statistic, do not ask for an affine invariant depth notion. The following task settings ask for different kinds of invariance.

- Affine invariance: general independence of coordinate system, e.g. in estimating parameters, testing hypotheses, and outlier identification.
- Weak affine invariance (= affine invariance up to a scalar constant): independence of coordinate system up to a homogeneous scale change.
- Orthogonal invariance: the set of Euclidean distances among pairs of points has to remain unchanged.
- Translation invariance: pure location problems and problems that depend on the specific meaning of the coordinate axes (e.g. length and weight).
- Invariance to coordinate-wise resp. uniform scaling: general dispersion problems resp. dispersion problems having a common measurement scale of coordinates (e.g. lengths of some object).
- Ordinal dissimilarity invariance: problems that depend on ordinal dissimilarity information only.
- Combinatorial invariance: outlier prone data that ask for a robust procedure.

## 3.2 Median and central regions

In particular, different notions of depth have different medians, which we will discuss next. Also, the shape of central regions and relations to lower-dimensional projections are of interest.

- Uniqueness of median A median (= point of maximum depth) may be unique or not. Mahalanobis depth is uniquely maximized at  $E[\mathbf{X}]$ , zonoid depth too. The halfspace median is unique if  $P$  has an L-density and connected support, but generally not; see also Prop. 7 in Mizera and Volauf (2002). Simplicial median is not unique either. The depth  $D_{L_2}$  takes its maximum at the *spatial median* (which in some literature unfortunately goes under the term  $L_1$  median); so does the spatial depth.

Onion depth is maximum at the innermost convex contour, and this maximum is generally non-unique. Under central symmetry the onion depth is obviously maximal at the center (but not under angular or halfspace symmetry).

Oja depth is maximum at the Oja median, which is not unique; see the **R**-package **OjaNP** (Fischer et al., 2020). The Oja median minimizes the average volume of simplices

$$\begin{aligned} & \binom{n}{d}^{-1} \sum_{1 \leq i_1 < \dots < i_d \leq n} \text{vol}_d(\text{conv}\{\mathbf{y}, \mathbf{x}_1, \dots, \mathbf{x}_d\}) \\ &= \frac{(n-d)!}{n!} \sum_{1 \leq i_1 < \dots < i_d \leq n} |\det((1, \mathbf{y}^\top)^\top, (1, \mathbf{x}_{i_1}^\top)^\top, \dots, (1, \mathbf{x}_{i_d}^\top)^\top)|. \end{aligned}$$

- Convex or star-shaped level sets:

Most depths have convex central regions, that is, are *convex unimodal* functions about their median. Among them are the Mahalanobis,  $\mathbb{L}_p$ , halfspace, simplicial volume and zonoid depths. On L-continuous angular-symmetric distributions, simplicial depth is *star unimodal* about the median, having starshaped central regions (Liu, 1990). The spatial depth does not satisfy monotonicity on rays; so it has neither convex nor starshaped level sets (Nagy, 2017).

- Projection property:

Some depths have the *projection property*,

$$D(\mathbf{y}|P) = \inf_{\mathbf{p} \in S^{d-1}} D(\langle \mathbf{p}, \mathbf{y} \rangle | P_{\mathbf{p}}), \quad \mathbf{y} \in \mathbb{R}^d, \quad (22)$$

where  $\mathbf{X} \sim P$  and  $P_{\mathbf{p}}$  is the distribution of the random variable  $\langle \mathbf{p}, \mathbf{X} \rangle$ , that is, of  $\mathbf{X}$  projected on a ray from 0 in direction  $\mathbf{p}$ . A depth that satisfies (30) possesses convex level sets.

The projection property (30) allows us to approximate a depth value from above by evaluating the univariate depth of projected data at a finite number of directions  $\mathbf{p}$  and taking the minimum. For example, the halfspace depth and the projection depth satisfy the projection property, as well as the zonoid depth and the Mahalanobis depth; see Dyckerhoff (2004).

### 3.3 Uniqueness and continuity

If a depth serves as part of a more complex statistical procedure, we may be interested in properties of it beyond empirical distributions.

- Population version:

Halfspace and simplicial depth have a population version for general distributions, while zonoid and Mahalanobis depth extend to distributions with finite first resp.

second moments. Mahalanobis depth, being a continuous function of moments, obviously satisfies a Law of Large Numbers; the same holds for halfspace depth (Donoho and Gasko, 1992), simplicial depth (Dümbgen, 1992), and zonoid depth (Mosler, 2002, Th. 4.6). However, convex hull peeling depth, being popular in data analysis, is restricted to empirical distributions.

- Information on  $P$ :

Another important feature of a depth is how much information it carries about the underlying distribution  $P$ , that is, how far  $P$  is identified, given  $D(\mathbf{y}|P)$  for all  $\mathbf{y}$ . While the Mahalanobis depth identifies the first two moments of  $P$  only, the zonoid depth fully determines  $P$ . Halfspace depth identifies the distribution uniquely if the distribution is either discrete (Koshevoy, 2002; Cuesta-Albertos and Nieto-Reyes, 2008b) or continuous with compact support (Koshevoy, 2003); see also (Nagy et al., 2019, Th. 34) and Nagy (2019). The Oja depth determines the distribution uniquely among those measures which have compact support of full dimension (Koshevoy, 2003). With simplicial depth holds the same for empirical distributions in general position (Koshevoy, 1997). If we restrict the analysis to a family of elliptically symmetric distributions having a common strictly monotone decreasing radial density, any affine-invariant depth  $D$  determines the distribution uniquely.

- Continuity on  $\mathbf{y}$  and  $P$ :

For numerical calculations it is important, that the depth depends continuously on the data, i.e., that  $D$  be continuous as a function of  $\mathbf{x}$  and weakly continuous on  $P$ , uniformly in  $\mathbf{x}$ . More precisely, for some class of distributions  $\mathcal{P}$  may hold:

$$\lim_{\mathbf{x}_n \rightarrow \mathbf{x}} |D(\mathbf{x}_n|P) - D(\mathbf{x}|P)| = 0 \quad \text{for any sequence } (\mathbf{x}_n) \text{ converging to } \mathbf{x}, \quad (23)$$

$$\lim_{n \rightarrow \infty} \sup_{\mathbf{x} \in C} |D(\mathbf{x}|P_n) - D(\mathbf{x}|P)| = 0 \quad \text{for any weakly converging } P_n \Rightarrow P \text{ in } \mathcal{P}. \quad (24)$$

Mahalanobis depth is continuous (23) on  $\mathbf{y} \in \mathbb{R}^d$  and meets (24) on distributions having a regular covariance matrix. Under a slight regularity condition (Casco and López-Díaz, 2016), zonoid depth satisfies (23) at every  $\mathbf{y} \in \mathbb{R}^d$  and (24) on distributions having finite first moment. The same holds for  $\mathbb{L}_2$  depth. Halfspace and simplicial depths are in general non-continuous. The latter depends continuously on  $\mathbf{y}$  and  $P$  if  $P$  has an L-density. Oja depth is obviously continuous on  $\mathbf{y}$  as well as on an empirical distribution  $P$ .

Table 2 summarizes the principal properties of the depth notions considered.

| Property  | $D_{Mah}$ | $D_{\mathbb{L}_p}$ | $D_H$  | $D_{Proj}$ | $D_{Sim}$ | $D_{Oja}$ | $D_{Zon}$ | $D_{Spa}$ | $D_{Lens}$ | $D_{Skel\beta}$ | $D_{onion}$ |
|---|-----------|--------------------|--------|------------|-----------|-----------|-----------|-----------|------------|-----------------|-------------|
| invariant w.r.t.:   |           |                    |        |            |           |           |           |           |            |                 |             |
| $\mathcal{T}_T \cup \mathcal{T}_O \cup \mathcal{T}_{uSc}$ | Y         | $Y_{p=2}$          | Y      | Y          | Y         | Y         | Y         | Y         | Y          | Y               | Y           |
| $\mathcal{T}_A$   | Y         | $Y_{p=2^w}$        | Y      | Y          | Y         | Yw        | Y         | Yw        | Yw         | Yw              | Y           |
| $\mathcal{T}_{Com}$                                       | N         | N                  | Y      | N          | Y         | N         | N         | N         | N          | N               | Y           |
| max at point of:  |           |                    |        |            |           |           |           |           |            |                 |             |
| central symmetry  | Y         | Y                  | Y      | Y          | Yc        | Y         | Y         | Y         | Y          | Y               | Y           |
| angular symmetry  | N         | $Y_{p=2^w}$        | Y      | Y          | Yc        | N         | N         | Y         | N          | N               | N           |
| halfsp. symmetry  | N         | $Y_{p=2^w}$        | Y      | Y          | Yc        | N         | N         | N         | N          | N               | N           |
| unique median   | Y         | Y                  | Yc     | Y          | Yc        | N         | Y         | Y         | N          | N               | N           |
| convex regions  | Y         | Y                  | Y      | Y          | N         | Y         | Y         | N         | N          | N               | Y           |
| starshaped regions  | Y         | Y                  | Y      | Y          | Yca       | Y         | Y         | N         | Ycs        | Ycs             | Y           |
| population version  | Y         | Y                  | Y      | Y          | Y         | Y         | Y         | Y         | Y          | Y               | N           |
| continuous on $\mathbf{y}$                                | Y         | Y                  | N      | Y          | Yc        | Y         | Y         | Y         | Yc         | Yc              | N           |
| continuous on $P$   | Y         | Y                  | N      | Y          | Yc        | Ye        | Y         | Y         | Y          | Y               | N           |
| uniqueness of $P$   | N         |                    | Yd, Yc |            | Ye        | Y         | Y         | Y         |            |                 | N           |
| projection prop.  | Y         |                    | Y      | Y          | N         |           | Y         | N         | N          | N               |             |

Table 2: Principal analytical properties of depth notions;  $d \geq 2$ . Y: Yes; N: No. Ya: Yes for angular symmetric  $P$ ; Ys: for centrally symmetric  $P$ ; Yc: for L-continuous  $P$ ; Yd: for discrete  $P$ ; Ye: for empirical  $P$ ; Yw: after whitening;  $Y_{p=2}$ : for  $p = 2$ . Regularity conditions like compact or full-dimensional convex support, uniform integrability of distributions, general position of data, etc are omitted.

## 4 Specifics of the data

Special aspects of the data can also guide us in selecting a particular depth notion. E.g., some properties of the data generation process may be known from the setting of the task, like symmetries or the proneness of the process to produce outliers. Further, parts of the data may be missing or be non-metrically scaled.

In principle, a data depth  $D(\mathbf{y}|\mathbf{X})$  is evaluated at the point  $\mathbf{y}$  and  $n$  points representing the support of  $\mathbf{X}$ , which data is usually given as a complete  $(n+1) \times d$ -matrix of real numbers. (Functional data may be treated, after proper discretization, like multivariate data.) However, some depth notions can cope with incomplete data, others even with ordinal ones.

When coordinate values of  $\mathbf{y}$  are missing, the depth calculation may be restricted to a lower-dimensional space of attributes, corresponding to the values that are non-missing. If the depth satisfies the projection property (30), this yields an upper bound of the unknown depth value.

When coordinate values are missing of points in the support of  $\mathbf{X}$ , a lower bound on zonoid depth  $D_{Zon}(\mathbf{y}|\mathbf{X})$  can be determined as follows. Let values of the  $j^*$ -th coordinate,

$x_{ij^*}$ , be missing at observation units  $i \in J \subset \{1, 2, \dots, n\}$ . If we impute, as usual, for each of the missing values the arithmetic mean  $\bar{x}_{j^*} = \text{ave}_{i \notin J} x_{ij^*}$ , a lower bound of the depth is achieved. To see this, note that in Formula (10) the restriction

$$y_{j^*} = \sum_{i=1}^n \lambda_i x_{ij^*}, \quad \text{that is} \quad y_{j^*} - \bar{x}_{j^*} = \sum_{i=1}^n \lambda_i (x_{ij^*} - \bar{x}_{j^*}),$$

arises. By the imputation, the latter summands with  $i \in J$  will become zero, so that at least one of the weights  $\lambda_i$  will decrease (in the weak sense), hence  $D_{Zon}(\mathbf{y}|\mathbf{X}) = \inf_i (n\lambda_i)^{-1}$  not be lowered.

If only ordinal information about distances is available, lens depth may be used, see Kleindessner and Von Luxburg (2017).

## 4.1 Symmetry

In many applications we have prior information on symmetries of the data generating process, which may yield data that are close to being point symmetric, angular symmetric, elliptically or spherically symmetric.

If the data follows an elliptical law, the central regions of every affine invariant depth will be ellipses and coincide with the density level sets. Under this assumption, Mahalanobis depth is completely satisfactory and also fast to compute. Moreover, under ellipticity, it is obvious that the level sets of any affine invariant depth coincide with the density level sets.

But observe that in general depth and density are genuinely different concepts. This is obvious for Mahalanobis regions when the the distribution is non-elliptic. For illustration, see Figure 3. It exhibits depth central regions and density level sets having the same probability content and being generated by a skewed bivariate Gaussian law (Azzalini and Valle, 1996), for Mahalanobis, Tukey and onion depth, and sample sizes  $n = 100, 1000, 10000$ .

Also a possible proneness of the data generation process to producing outliers may be typical in a given task. For robustness, see the next Section 4.2.

## 4.2 Possible outliers

If the data is suspected to be contaminated by outliers, we may be interested in a robust procedure that reduces the influence of outliers in an automatic, built-in way. Several notions of depth are known to be more or less suitable to downsize the weight of possibly outlying data.

If we expect that outliers may occur, a robust depth notion should be used. A combinatorial depth, like halfspace or simplicial depth, is robust but comes at considerable computational cost. If ellipticity (except outliers, of course) is assumed, we may employ

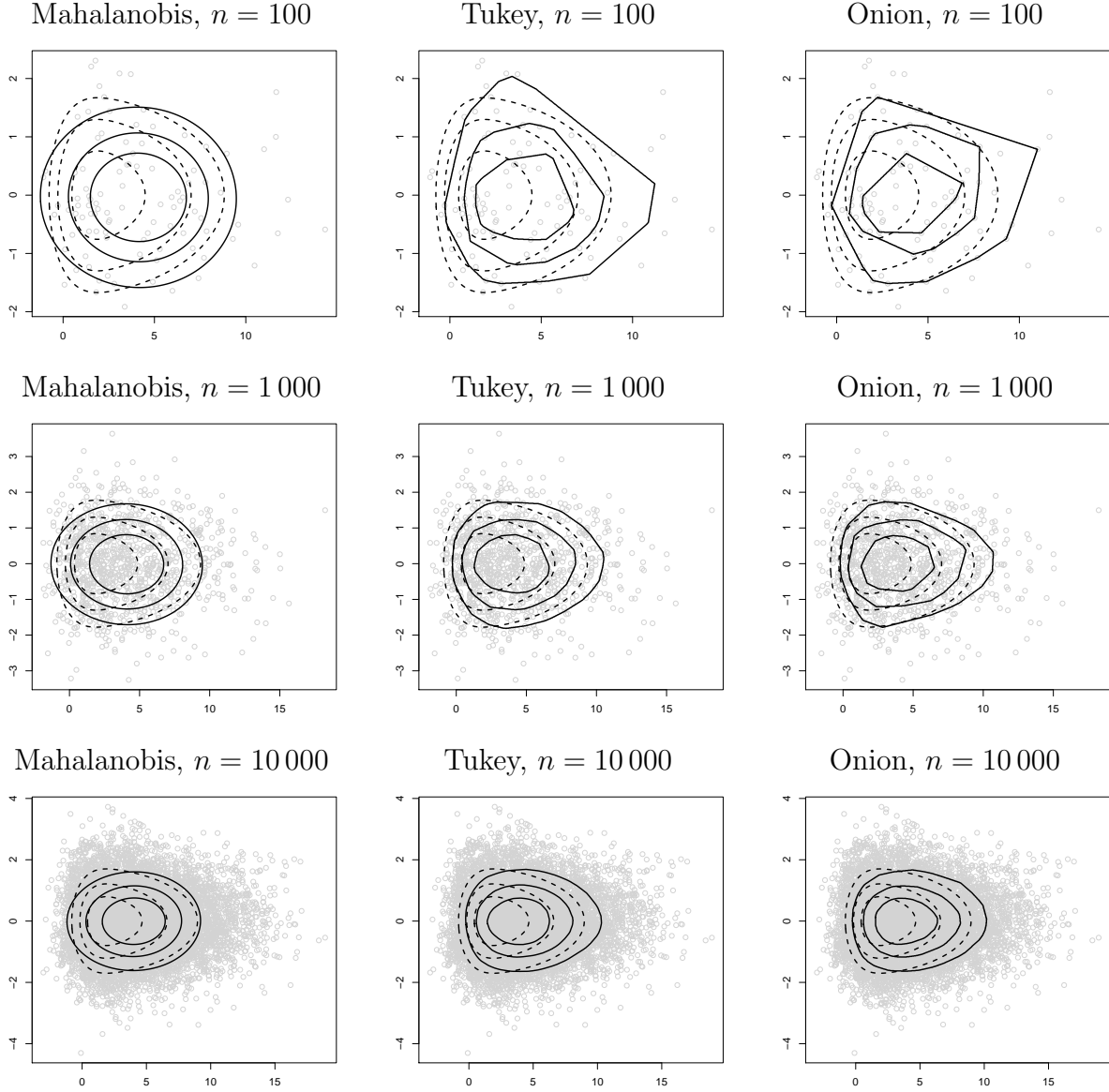


Figure 3: Comparison of three depth (solid lines) and density (dotted lines) contours for a bivariate skewed normal distribution. The contours encompass 0.75, 0.5 and 0.25 deepest resp. densest points. Mahalanobis (left column), Tukey (middle column) and onion (right column) depths for a sample of  $n = 100$  (top row), 1 000 (middle row) and 10 000 (bottom row) points.



the Mahalanobis depth with a robust covariance estimate (e.g. MCD), which is computationally much cheaper. Spatial depth is robust as well, and fast to compute, but not affine invariant, which can be healed by a robust scatter transformation, see Section 3.1 above. Figure 4 exhibits central regions of several depths when the data are subject to an MCD scatter transformation. However, note that plugging-in a robust scatter estimator in place of the usual covariance matrix can influence the stochastic properties of the depth statistic; see Nordhausen and Tyler (2015).

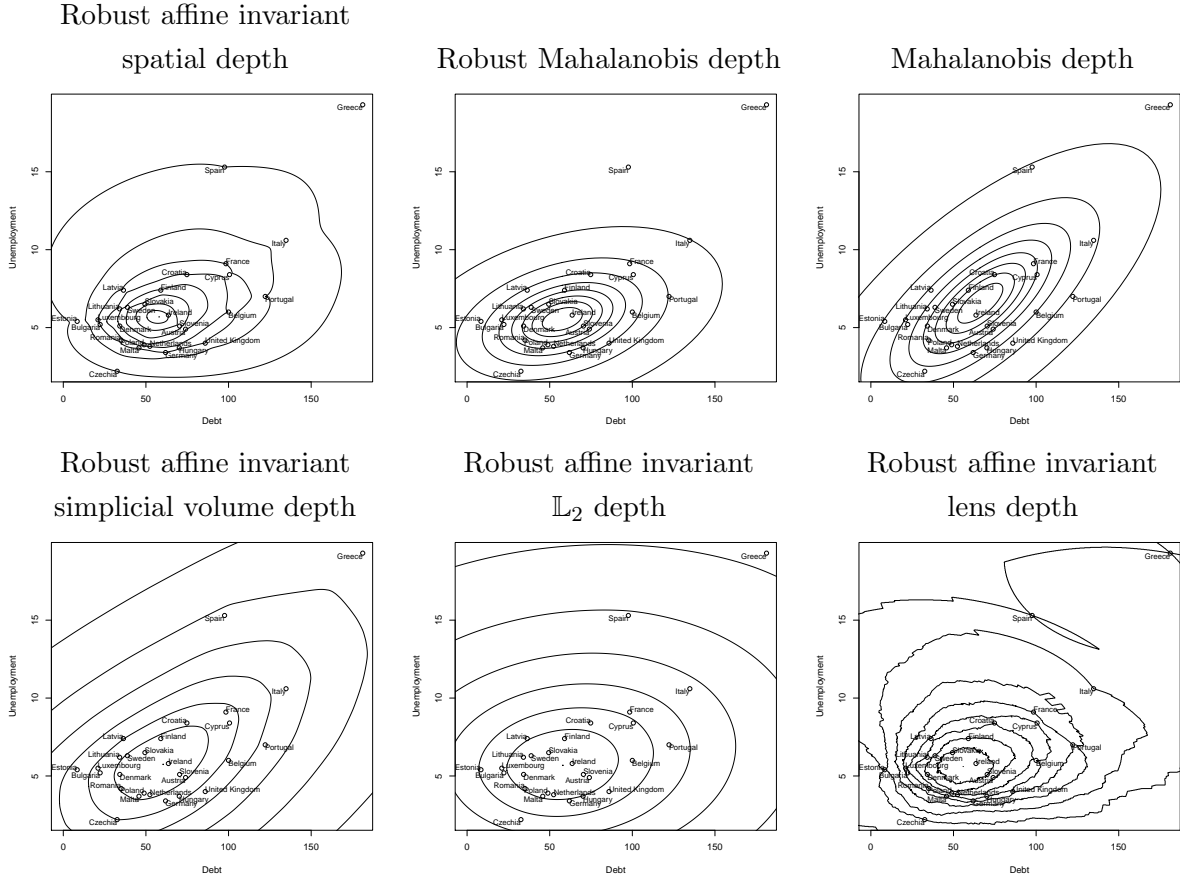


Figure 4: Central regions of EU data on unemployment and public debt in 2018 (Source: EUROSTAT): Five notions of depth, made affine invariant by using a robust scatter matrix (MCD with parameter  $\alpha = .75$ ); for comparison (upper right panel), the non-robust Mahalanobis depth, being calculated with the usual covariance matrix.

An indicator of the robustness of a depth is the asymptotic breakdown point of its median. It forms an upper bound of the breakdown of any depth region. The breakdown of the Tukey median is at least  $1/(d + 1)$  (Donoho and Gasko, 1992, Prop. 3.4). The Oja median possesses breakdown 0 (Niinimaa et al., 1990), hence all simplicial volume regions

have breakdown 0. The same holds for onion regions (Donoho and Gasko, 1992, Sec. 4). Also, zonoid regions and, more general, weighted mean regions have breakdown 0 as their median equals the mean of the data. The breakdown of the  $\mathbb{L}_2$ -depth median (= spatial median =  $\mathbb{L}_1$  median) is  $1/2$  (Lopuhaa et al., 1991). However the breakdown of the depth function  $D_{\mathbb{L}_p}(\mathbf{y})$  at some point  $\mathbf{y}$  can be much higher (Zuo, 2004). Another indicator of robustness of a depth is the influence function of its median; it is investigated in Romanazzi (2001) for halfspace depth, in Niinimaa and Oja (1995) for  $\mathbb{L}_2$ -, spatial, and Oja depth, in Zuo (2004) for  $\mathbb{L}_p$  depth, and in Zuo (2006) for projection depth.

Also, the direction of outliers can be relevant. If we are interested in the direction of an outlier, we may employ a non-robust depth that (like the zonoid depth) possesses the projection property. Then a point can be identified as an outlier, if it has low depth value, minimized over the relevant directions.

### 4.3 A study of different depths in classification

To study depth performance in different settings, the  $DD\alpha$ -classifier (Lange et al., 2014b) is applied to classification problems in dimensions two and three.

Consider a random vector,  $Z$ , from one of the following distributions: standard normal distribution; spherical Student  $t$ -distribution with five degrees of freedom; spherical Cauchy distribution; uniform distribution on square resp. cube; skewed-normal distribution with skewness parameter equal to five in the first coordinate according to Azzalini and Valle (1996); product of independent univariate exponential distributions having parameter 1.

First, location alternatives are constructed. The two classes correspond to  $X_1 \stackrel{d}{=} \boldsymbol{\mu}_1 + Z$  and  $X_2 \stackrel{d}{=} \boldsymbol{\mu}_2 + Z$ , where  $\boldsymbol{\mu}_1 = (0, 0)^\top$ ,  $\boldsymbol{\mu}_2 = (1, 0)^\top$  in dimension  $d = 2$  and  $\boldsymbol{\mu}_1 = (0, 0, 0)^\top$ ,  $\boldsymbol{\mu}_2 = (1, 0, 0)^\top$  in dimension  $d = 3$ . Training and test samples include twice 100 and twice 500 observations, respectively. Samples from the two classes, for each of the six classification problems in dimension two, are illustrated in the Supplementary Material.

The  $DD\alpha$ -classifier is obtained in two steps: First each training point is represented by its depth values regarding the two training classes, which results in a two-dimensional  $DD$ -plot. Then, by the  $\alpha$ -procedure, a rule is determined that separates the training points in the  $DD$ -plot. New items are similarly represented and then classified by the  $DD\alpha$ -rule. For details, see Lange et al. (2014b).

Boxplots of the error rates on the two-dimensional classification problems are constructed over 100 runs and contrasted with those of the optimal Bayes rule, which assigns a new point to the class of higher population density. See the Supplementary Material, where also tables of the medians and median absolute deviations are provided. The same is done for the three-dimensional problems. The projection depth is approximated by using 1000 directions, all other depths are exactly computed.

Obviously, a point that has depth 0 regarding both classes, a so called *outsider* (Lange

et al., 2014b), cannot be classified by the  $DD\alpha$ -rule. In our study we neglect outsiders and measure the classification error on the remaining points only. Note that the halfspace, simplicial, zonoid and onion depths vanish outside the convex hull of the data. For a fair comparison, the classification error for all the depths is measured only for points located inside the convex hull of at least one of the training samples.

The simulation study reveals that for our location alternatives in dimension two the best depth-based error rate is generally not far from the optimal Bayes rate. More precisely, the differences in median range from 0 for uniform data to three percent for Cauchy data. Things look only slightly worse in dimension three: Here differences between those medians vary from null in the uniform case to four per cent in the exponential case. Note that the first three alternatives (normal,  $t_5$ , Cauchy) consist of unimodal elliptical distributions differing in location. For those alternatives follows from Theorem 2 in Lange et al. (2014b) that the error rate of the  $DD\alpha$ -classifier converges to the optimal Bayes rate when the size of the training classes goes to infinity. The same follows for the uniform alternative from Theorem 1 in Lange et al. (2014b). For the other two alternatives (skewed normal, exponential) we have no such theoretical results.

Further, our results demonstrate that there exists no uniformly best choice of the depth notion. On uniformly distributed data all depths perform equally well. With other data slight differences prevail. When the data are elliptically symmetric (normal, Student, and Cauchy cases) onion depth, simplicial depth and Tukey depth appear to be less recommendable, similarly zonoid depth, when the data are prone to outliers (Cauchy case). Asymmetric data (as in the skewed and exponential cases) are worse classified with simplicial, lens, projection and Mahalanobis depth. Consequently, for the considered location alternatives, three depths show an overall acceptable behavior, *viz.* the Oja, spatial, and  $\mathbb{L}_2$  depths.

Next we study the classification of data that differ additionally in scale. Based on the above location alternatives, six location-scale alternatives are generated by multiplying the last coordinate of the second class with 2. The simplicity of this setting is explained by the affine invariance of all depths considered. The parameters of the simulation and the  $DD\alpha$ -procedure are the same as above. Box plots of error rates are obtained as before. For an illustration of the location-scale alternatives and for detailed results, see the Supplementary Material.

It comes out that the depth-based classification of location-scale alternatives, like that of pure location alternatives, yields median error rates that come close to the optimal Bayes rates. This means, with the best choice of depth we get error rates that usually differ just by one or two percent from the Bayes rate, and by at most four percent.

Again, there exists no uniformly best depth. But our results give an idea of the appropriateness of different notions. When the location-scale alternatives include elliptically

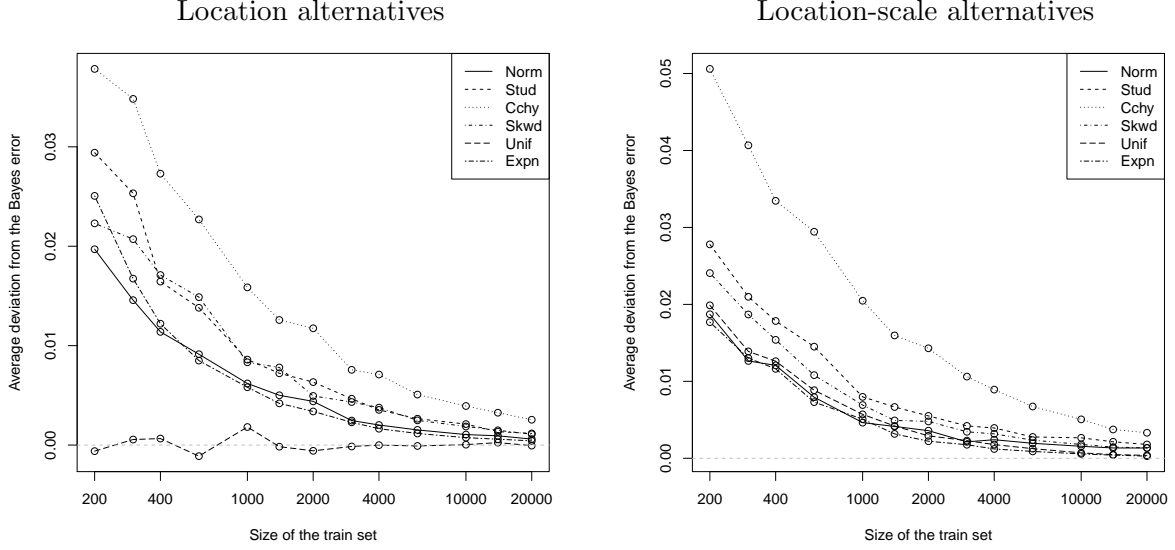


Figure 5: Average difference between the error rate of the  $DD\alpha$ -classifier (using halfspace depth) and the optimal Bayes rate when observations are increased; location alternatives (left), location-scale alternatives (right).

symmetric distributions, Tukey, onion, simplicial and zonoid depth seem to perform worse than others. With asymmetric data also simplicial and Mahalanobis depth operate more poorly. So, for this sort of location-scale alternatives, the remaining depths, *viz.* the lens, Oja, the spatial and the  $\mathbb{L}_2$  depth show an overall satisfactory behavior.

To further investigate an eventual convergence to the optimal Bayes rate, we increase the number of observations. Training observations total from 200 up to 20000, and five times more observations than trained are tested. Figure 5 exhibits, for each of the two-dimensional settings considered above, the difference (on an average, over 100 runs) between the observed error rate and the Bayes rate. We restrict the presentation to the halfspace depth.

One observes that in all cases the  $DD\alpha$  error rate decreases and approaches the Bayes rate when the number of observations increases. (An exception is the uniform location alternative, where the error rate always comes close to the Bayes rate.) While convergence for the first four location alternatives follows from theory, it is new for the remaining eight ones. Note that, in our implementation, the  $DD\alpha$ -classifier for separating the  $DD$ -plot employs polynomials whose degree is bounded by three. Li et al. (2012) provide further theoretical results and examples how classification in the  $DD$ -plot can produce error rates that come close to the base rate. This gives hope that depth-based classifiers can be of use in a rather wide range of applications, also beyond elliptically symmetric distributions.

## 5 Computational feasibility

For most notions of data depth, the depth of a point can, in principle, be exactly calculated. But the computational work increases with  $n$  and, often exponentially, with  $d$ ; the latter is typical for combinatorial depths. Then, practical restrictions on computation time and storage space may urge us to rely on approximative approaches. If  $n$  is large, thinning the data cloud (by random selection) may solve the task. To cope with a large dimension  $d$  comes out to be the much harder problem.

### 5.1 Exact calculations

Exact procedures have been implemented in the R-package `ddalpha` to calculate the following nine data depths: Mahalanobis,  $\mathbb{L}_2$ , spatial, zonoid, lens, onion, halfspace, simplicial volume, and simplicial depth. Note that for most of these depths the naive direct calculation is not feasible, and more sophisticated procedures of lower computational complexity have to be used.

For example, let us take a look at the halfspace depth. Its definition suggests a simple idea: splitting the sample in two parts and checking whether the parts can be linearly separated by a hyperplane containing  $\mathbf{y}$ . Then, among all partitions separable by a hyperplane, the one is selected that has the smallest number of observations on one side. However, there is a total of  $2^n$  possible partitions, which leads to a time complexity exponential in  $n$ . A closer inspection (Dyckerhoff and Mozharovskiy, 2016) gives an idea how to reduce the set of possible candidates, leading to an algorithm with polynomial complexity in  $n$ ,  $O(n^{d-1} \log(n))$ .

Figure 6 exhibits average computation times for each of the depths, depending on sample size  $n$  and dimension  $d$ , where  $n$  runs up to 1000 and  $d = 2, 3, 4, 5$ . Given  $n$  and  $d$ , 30 samples have been drawn, depth has been calculated for 25 points of each sample, and an average has been taken over these 25 points and 30 samples.

All calculations have been performed by means of the R-package `ddalpha` on a machine having processor Intel(R) Core(TM) i7-4980HQ (2.8 GHz) with 16 GB of physical memory and macOS Sierra (Version 10.13.4) operating system.

As we see from Figure 6, the depth notions differ greatly in their computation times, some sharply increasing with  $n$  and  $d$ . (In each panel, times and sample sizes are measured on a double logarithmic scale.) Table 3 lists the complexities of the various algorithms, including references to the literature.

- Mahalanobis depth and  $\mathbb{L}_2$  depth, as well as spatial depth, are always quickly calculated, and their computation times are virtually independent of (moderate values of)  $n$  and  $d$ .

- In dimension  $d = 2$  all depths can be sufficiently fast calculated, with times staying below 100 milliseconds even w.r.t. a sample of  $n = 1000$  points.
- When  $d \geq 3$ , the two combinatorial invariant depths, simplicial and halfspace depth, need much more computation time  $t$ , and at given dimension this time grows with  $n$  as  $t = n^{const_d}$ . The increase in  $d$  is exponential, see Table 3 regarding computational complexity. The same holds for the simplicial volume depth. Of these three depth notions, the simplicial depth is uniformly slowest, while the halfspace depth outperforms the other two. This experimental result corresponds to the respective complexities of order  $n^{d+1}$ ,  $n^d$ ,  $n^{d-1} \log(n)$ ; see Table 3.
- The time needed for the zonoid depth grows much slower with  $n$  and only slightly with  $d$ .
- The onion depth needs always more time than the zonoid depth, but has similar growth behavior.

| Depth notion      | Exact  | Approximate   |
|-------------------|--|---|
| Mahalanobis       | $O(n)$   | —   |
| $\mathbb{L}_p$    | $O(n)$   | —   |
| halfspace         | $O(n^{d-1} \log(n))$ , $O(n^d)$<br>Rousseeuw and Struyf (1998) | $O(kn)$<br>Dyckerhoff (2004)                              |
| projection        | $O(n^d)$ , Liu and Zuo (2014)                                  | Mozharovskiy et al. (2015)<br>$O(kn)$ , Dyckerhoff (2004) |
| simplicial        | $O(n^{d+1})$   | $O(k)$ number-approx.<br>$O(n^{d+1})$ portion-approx.     |
| simplicial volume | $O(n^d)$   | $O(k)$ number-approx.<br>$O(n^d)$ portion-approx.         |
| zonoid            | Dyckerhoff et al. (1996)                                       | $O(kn)$ , Dyckerhoff (2004)                               |
| Spatial           | $O(n)$   | —   |
| $\beta$ -skeleton | $O(n^2)$   | $O(k)$  |
| onion             | $O(n^{\lfloor d/2 \rfloor} / d^d)$ , Barber et al. (1996)      | —   |

Table 3: Time complexities for exact and approximate computation of several depths (of a given point in  $\mathbb{R}$  regarding a sample). For approximate computation,  $k$  stands for the number of random directions for halfspace, projection and zonoid depth, resp. for the number of considered simplices for simplicial and simplicial volume depth, resp. for the number of considered pairs of points for  $\beta$ -skeleton depth.

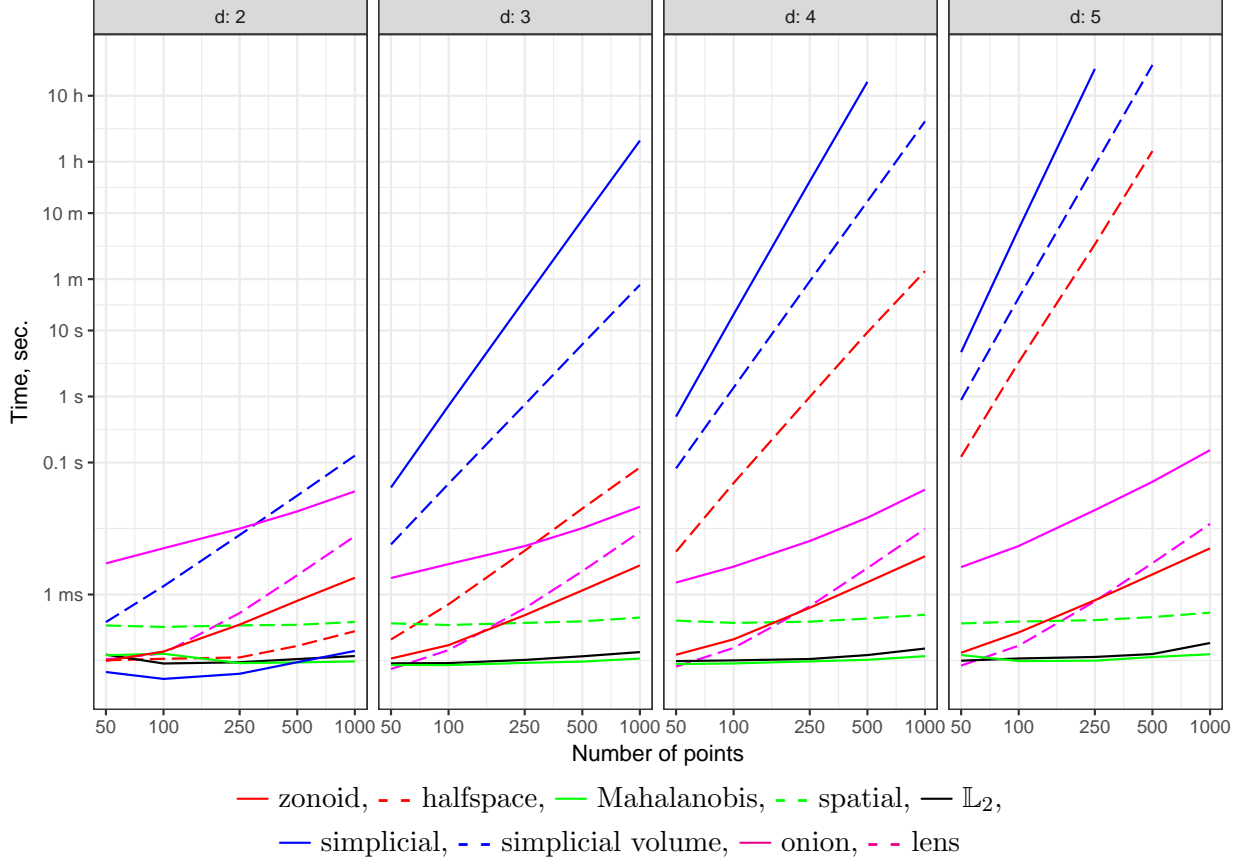


Figure 6: Calculation time of various depth functions on double logarithmic scale (sample size  $n$  and time  $t$ ).

Mostly, there is a trade-off between the accuracy of a procedure and its speed. As we see from Table 3, Mahalanobis,  $\mathbb{L}_p$ , and spatial depth have the best possible time complexity  $O(n)$  (as one cannot consider all points without looking at least once at each of them). Also, exact algorithms for zonoid (linear programming, which is known to be usually efficient) and  $\beta$ -skeleton depths are sufficiently fast; see Figure 6. A rather paradoxical result appears, when the Tukey depth of all points of a given sample is calculated with respect to the same sample. In this case, the complexity of computing the depth of a single point is lower than linear in  $n$ , *viz.*  $O(k \log(n))$ . For details see Section 2.3 of Mozharovskiy et al. (2015).

## 5.2 Approximate calculations

Clearly, if an exact procedure is available and time and memory space allow, the depth of a point should be calculated by the exact procedure. This is the obvious “gold standard”. However, it may be non-feasible in practice if  $d$  and/or  $n$  are too large or if the depth has to be very often evaluated

- as in bootstrap or permutation procedures, or
- when a whole central region is calculated.

Simplicial and simplicial volume depths can be approximated by considering either a fixed number or a constant portion of all simplices; in the latter case the complexity amounts to that of the exact algorithm, though. The respective complexities are exhibited in Table 3. To determine the onion depth in higher dimensions, the convex hull can often only be approximately calculated. This may yield ambiguous results and affect the computation of the onion depth.

If a depth satisfies the projection property (30) it may be approximated by using a finite set  $S \subset S^{d-1}$  of directions and taking the minimum, thus yielding an upper bound:

$$D^{\text{approx}}(\mathbf{y}|P) = \min_{\mathbf{p} \in S} D(\langle \mathbf{p}, \mathbf{y} \rangle | P_{\mathbf{p}}), \quad \mathbf{y} \in \mathbb{R}^d \geq D(\mathbf{y}|P) \quad (25)$$

Not every depth satisfies the projection property, and thus can be approximated with random directions. Some depths have non-convex regions, like the spatial and the simplicial depth, some need drawing simplices, like the Oja depth and the simplicial depth. The approximation from above may, in particular, be worthwhile for the halfspace depth and the projection depth. (Recall that Mahalanobis and zonoid depth can be exactly calculated at low cost.)

If information about ‘favourable’ directions is known, these directions should be primarily pursued. If not, directions are randomly chosen on the unit sphere, which is known as the *random Tukey depth* (Cuesta-Albertos and Nieto-Reyes, 2008a). However, the number of directions needed for a given precision is not known; for some results on convergence rates, see Nagy et al. (2019).

Figure 7 shows how often an approximation by the random Tukey depth (RTD) hits the correct value of the Tukey depth if we choose just 1000 random directions. While in dimension  $d = 2$  this is virtually always the case, in dimension  $d = 3$  (resp.  $d = 4$ ,  $d = 5$ ) the portion of correct values decreases with the sample size  $n$ , attaining less than 50 percent resp. 25 percent at  $n = 300$ . Presumably, the number of needed directions goes exponentially with  $d$ ; see also Cuesta-Albertos and Nieto-Reyes (2008a). However, e.g. for normally distributed data and number of directions fixed to 1000, relative and absolute errors stay rather small up to dimension  $d = 5$ ; see the Supplementary Material.

However, if we are interested in a most precise value of a depth statistic, it may often be computationally cheaper to calculate the exact depth immediately instead of repeatedly seeking for approximate values.

In certain applications many depth values have to be determined, while the precision of each single value is less important. E.g. in depth-based classification the rule is noisy



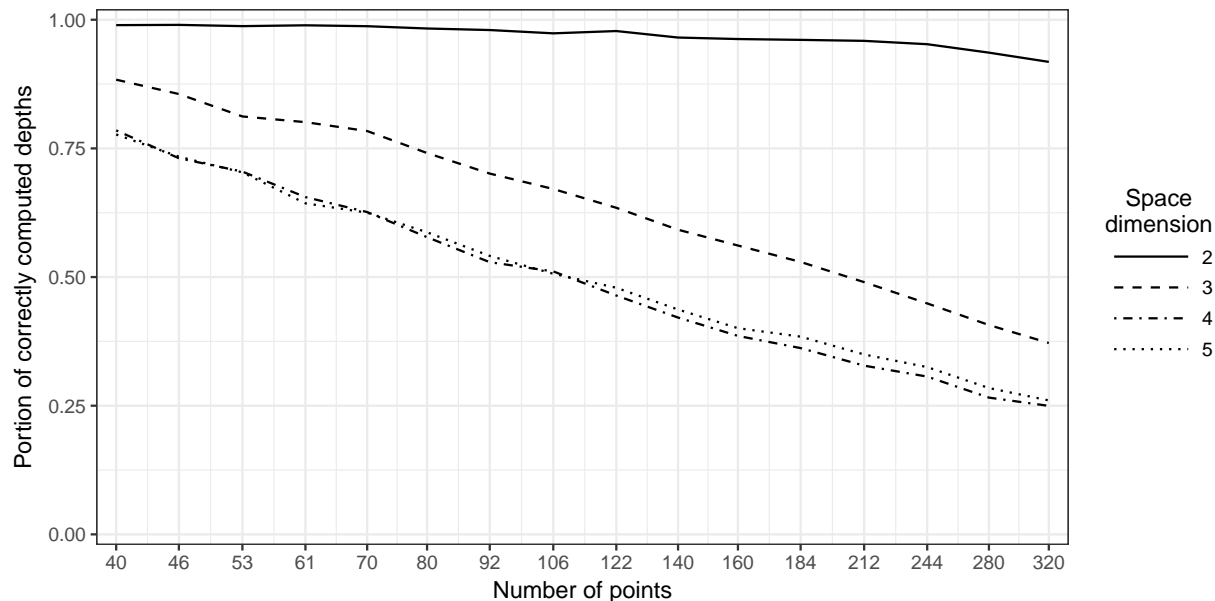


Figure 7: Average rates of achieving the exact value of Tukey depth when calculating the random Tukey depth at 1000 directions. The directions are uniformly distributed on the unit sphere, and the average is taken over all points of a standard normal sample with respect to the remaining sample, given  $d$  and  $n$ .

anyway, so the noise from the approximation may not much influence the results of cross-validation and the finally constructed rule (if at all); see e.g. Lange et al. (2014a). To give another example, in nonparametric testing based on data depth (Dyckerhoff, 2002), the Wilcoxon-Mann-Whitney ranks do not very sensibly depend on the single depth values. In these and many other applications the precision of the depth calculation must be related to the noisiness of the remaining procedure, and more or less rough approximations may be well.

### 5.3 Implementations

Data depths have been implemented in several existing software packages. In particular, R-package `ddalpha` (Pokotylo et al., 2019, 2020) implements exact procedures for all above mentioned depths, except projection depth. In addition, approximate algorithms are provided for the halfspace, projection, simplicial, and simplicial volume depths. Packages `depth` (Genest et al., 2017), `DepthProc` (Zawadzki et al., 2020), `fda.usc` (Febrero-Bande and Oviedo de la Fuente, 2012), `mrfDepth` (Segaert et al., 2019) implement a number of depth notions as well.

Mahalanobis depth is easily coded by hand in any programming language; ready-to-use implementations are also found in R-packages `DepthProc` and `fda.usc`. R-package

`DepthProc` suggests an implementation of  $\mathbb{L}_p$  depth. Halfspace depth can be computed exactly for  $d \leq 3$  (and approximately) in any dimension with R-packages `depth` and `mrDepth`, and only approximately with R-packages `DepthProc` and `fda.usc`. Exact projection depth is computed with MATLAB-package `CompPD` (Liu and Zuo, 2015), while approximate procedures are included in R-packages `DepthProc`, `fda.usc`, and `mrDepth`. Exact simplicial depth for  $d = 2$  is calculated with R-packages `depth`, `fda.usc`, and `mrDepth`. Exact simplicial volume depth is also computed using R-package `depth`. Spatial depth is implemented in R-package `depth.plot` (Mahalanobish and Karmakar, 2015).

Obviously, this overview cannot be complete. Moreover, the packages are continuously modified by their authors.

## 5.4 Large and high-dimensioned data

Depth statistics can also be applied to analyse sets of data having large data size  $n$  and/or high dimension  $d$ . But the different notions of depth are appropriate to different situations, and sometimes a pre-treatment of the problem may be needed.

Computational feasibility of a depth notion depends on  $n$  and  $d$  as well as on their relative size. In most applications  $n$  is considerably larger than  $d$ ,  $n \gg d$ . If not, a large portion of data lies on the border of the data cloud's convex hull and, consequently, has zero depth in all depth statistics that vanish outside this convex hull, *viz.* halfspace, simplicial, zonoid and onion depth, which idles these notions. If  $n < d$  or the sample covariance matrix is ill-conditioned, Mahalanobis depth as well as other whitened depths have to be modified by basing them on another shape matrix.

If both  $n$  and  $d$  are large and  $n > d$ , Mahalanobis depth can routinely be calculated, while for moderate  $d$  zonoid, spatial, lens, and  $\mathbb{L}_p$ -depth are computationally feasible. However if the properties of these depths do not fit to the application problem at hand, we may reduce  $n$  and/or  $d$ .  $n$  is decreased by ‘thinning’, that is selecting a representative part of the sample. To downsize  $d$ , ‘features’ (= attributes of the sampled items) have to be preselected by recurring to additional information.

## 6 Local and functional depths

This section shortly discusses two extensions of the above: depth notions that reflect local properties (like multiple modi) of the distribution, and depth notions for functional data.

### 6.1 Local depths

As we have observed in Section 4.1, depth and density are different concepts. The reason is that depth refers to the whole distribution, while density measures it locally. In some

instances a kind of depth is asked for which describes local aspects of the distribution. Agostinelli and Romanazzi (2011) introduce localized versions of Tukey and simplicial depth. For Tukey depth, they replace the halfspaces in Definition (4) with infinite slabs of finite width  $h$ , for simplicial depth they restrict to simplices of some given volume  $h$ . When  $h$  goes to infinity, the usual notion is obtained. The smaller  $h$ , the more local features of the distribution are represented by the depth.

A depth that is based on point differences, like the spatial depth and the Mahalanobis depth, can be localized as follows: Transform each difference  $\mathbf{t}$  by a positive definite kernel,  $k_h$ , e.g. the Gaussian kernel  $k_h(\mathbf{t}) = (\sqrt{2\pi h})^{-d} \exp(-\|\mathbf{t}/h\|^2/2)$ , and calculate the respective *kernelized depth*. By this approach, Chen et al. (2009) introduce the *kernelized spatial depth*:

$$D_{kSpa}(\mathbf{y}|\mathbf{X}) = E[k_h(\mathbf{y} - \mathbf{X})] - \left\| E \left[ k_h(\mathbf{y} - \mathbf{X}) \cdot \frac{\mathbf{y} - \mathbf{X}}{\|\mathbf{y} - \mathbf{X}\|} \right] \right\|. \quad (26)$$

$D_{kSpa}^*$  is obtained by first whitening  $\mathbf{y} \cup \mathbf{X}$  and then kernelizing the distances. It, up to scale, approaches density (resp. usual spatial depth), when the band width  $h$  goes to 0 (resp.  $\infty$ ); see (Dutta et al., 2016, Theorem 3). A kernelized Mahalanobis depth is proposed by Hu et al. (2011).

Different from these approaches, Paindaveine and Van Bever (2013) construct a local depth by conditioning a given (global) depth  $D(\mathbf{y}|\mathbf{X})$  on a neighborhood of  $\mathbf{y}$ . Instead of the distribution  $P_{\mathbf{X}}$  of  $\mathbf{X}$ , they consider the mixture  $P_{\mathbf{y},\mathbf{X}} = .5P_{\mathbf{X}} + .5P_{2\mathbf{y}-\mathbf{X}}$ , which is a symmetric distribution about  $\mathbf{y}$ . For some probability  $\beta \in ]0, 1]$ , the central region  $D_{\beta}(P_{\mathbf{y},\mathbf{X}})$  serves as a local neighborhood of  $\mathbf{y}$ . Conditioning the global depth  $D(\mathbf{y}|\mathbf{X})$  on this neighborhood yields its  $\beta$ -*localized depth*,

$$D_{\beta}(\mathbf{y}|\mathbf{X}) = D(\mathbf{y}|P_{\beta,\mathbf{y},\mathbf{X}}), \quad (27)$$

where  $P_{\beta,\mathbf{y},\mathbf{X}}$  is the conditional distribution of  $\mathbf{X}$ , conditioned on  $D_{\beta}(P_{\mathbf{y},\mathbf{X}})$ . If  $D$  is affine invariant, so is its  $\beta$ -localized depth. Obviously, if  $\beta = 1$ , the global depth is obtained. If  $\beta \rightarrow 0$ , the localized depth  $D_{\beta}(\mathbf{y}|\mathbf{X})$  does *not* converge to the density of  $\mathbf{X}$  but rather to a constant which is positive and reflects local asymmetry for  $\mathbf{y}$  within the support of  $\mathbf{X}$ , and which (usually) vanishes outside.

As we see from Figure 8, localization is able to improve the fit of a multimodal distribution. On the other hand, spurious high-depth zones can arise (here, one for the bimodal and four for the trimodal data), due to the centrality-proneness of depth. For more examples, see the Supplementary Material. In applications the localization parameter has to be properly chosen, depending on the data and the problem at hand. This requires prior information or (e.g. in supervised classification) tuning.

An alternative to calculating a local depth at a given point is estimating its density value through a proper kernel estimate; this proves useful in *DD*-plot-like classification (Pokotylo and Mosler, 2019).

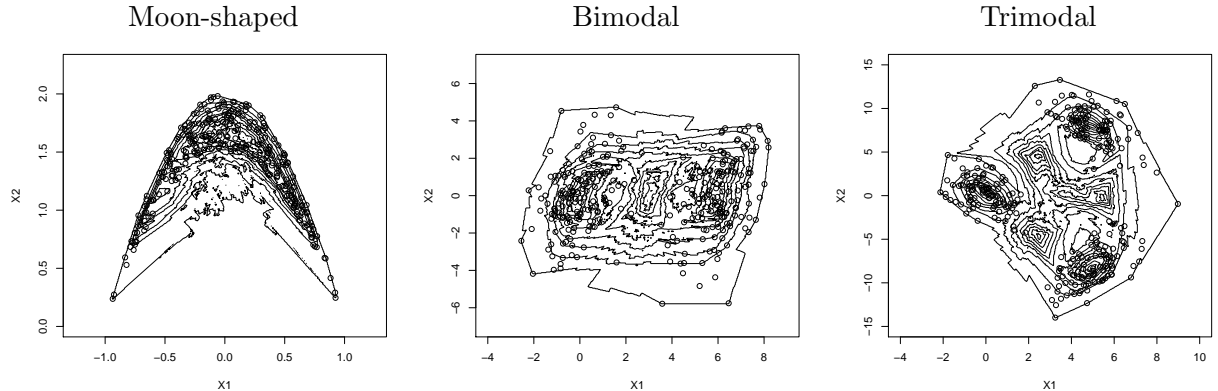


Figure 8: Central regions of  $\beta$ -localized halfspace depth, with localization parameter  $\beta = 0.33$ , for samples from moon-shaped (left), bimodal (middle) and trimodal (right) distributions.

## 6.2 Functional depths

So far, we have restricted our discussion to multivariate depths. However, notions of depth for functional data have gained much interest in the past decade. Consider a space  $E$  of functions  $[0, 1] \rightarrow \mathbb{R}^m$  equipped with the supremum norm and  $E'$  its dual space of continuous linear functions  $E \rightarrow \mathbb{R}^m$ . A functional data depth is a real-valued functional that measures how deep a function  $\mathbf{y} \in E$  is located in a given finite cloud  $\mathbf{X} = \{\mathbf{x}^1, \dots, \mathbf{x}^n\}$  of functions  $\in E$ . Several notions of functional depth have been proposed in the literature; for a survey on their properties, see Gijbels and Nagy (2017). Most known functional depths belong to two types, which build on multivariate depths like those discussed above. Either they are of *integral type* (Nagy et al., 2016),

$$D(\mathbf{y}|\mathbf{X}) = \int_0^1 D^m(\mathbf{y}(t)|\mathbf{X}(t))dt, \quad (28)$$

or of *infimum type* (Mosler and Polyakova, 2012)

$$D(\mathbf{z}|\mathbf{X}) = \inf_{\varphi \in \Phi} D^m(\varphi(\mathbf{y}|\varphi(\mathbf{X}))), \quad (29)$$

where  $D^m$  is an  $m$ -variate data depth,  $\Phi$  is a proper subset of linear functionals in  $E'^d$ , and  $\varphi(\mathbf{X})$  is the transformed data cloud  $\{\varphi(\mathbf{x}^1), \dots, \varphi(\mathbf{x}^n)\}$ . Population versions are similarly defined.

A depth of integral type (28) is just an average of multivariate depth values attained at all ‘times’  $t$ . Note that in definition (29) of infimum-type depth each  $\varphi$  may be interpreted as a particular aspect of  $\mathbf{y}$  we are interested in and which is represented in  $m$ -dimensional

space. A depth of infimum type (29) is given as the smallest multivariate depth of  $\mathbf{y}$  under all these aspects.

It is obvious from definitions (28) and (29) that the properties of these functional depths depend essentially on the properties of the involved multivariate depth. For a comprehensive treatment, we refer to Gijbels and Nagy (2017).

## 7 Concluding remarks

Several popular notions of multivariate depth functions have been considered and compared, with a view to practical applications. Different depths yield different central (= trimmed) regions and different medians. While many notions are affine invariant and, thus independent of a coordinate system, some are only rigid-body invariant (regarding translation and orthogonal transform), but can be made affine invariant through whitening the data. The depth notions differ in their analytical properties, particularly in the information they carry about the underlying distribution and its center. E.g., the zonoid depth characterizes the whole distribution, while the Mahalanobis depth determines the first two moments only. Also, for numerical calculations, continuity is an issue. Some notions (like halfspace and simplicial depth) are robust against extremely outlying data, others are not. These and several other properties must guide the choice of a proper depth notion in a specific application.

Moreover, as all depth notions (besides moment Mahalanobis depth) are more or less computationally intensive, computational feasibility is a key aspect in this choice. For all notions considered here, exact and/or approximate algorithms exist, which are implemented in R-packages like `ddalpha`. But computational complexity of these procedures ranges from  $O(n)$  to  $O(n^{d+1})$ . These complexities have been presented above together with calculation times of exact procedures for moderate  $n$  and  $d$ .

A prominent application of depth statistics is classification (= supervised learning). A numerical study has been given that compares various depths regarding their error rates in classifying data to several location and location-scale alternatives.

For some depths on higher-dimensional data and larger sample sizes, approximate algorithms have to be employed. Their complexities are given above as well. Regarding the accuracy of approximate procedures, specifically the random Tukey depth has been numerically compared with the exact halfspace (= Tukey) depth, using a fixed number of random directions. General strategies for large and high-dimensioned data have been discussed, too.

Many of these remarks apply also to depth statistics for functional data, as the functional depths usually build on multivariate depth notions and operate on discretized versions of the data.

We close with a few rough recommendations to the practitioner of data analysis.

1. For large data sets, spatial,  $\mathbb{L}_2$ , and Mahalanobis depths can be efficiently and exactly calculated. Next to them, lens and zonoid depths.
2. Most real data are far from being elliptically shaped. Such data should *not* be treated with Mahalanobis depth, but with a depth that reflects the given shape of the data (and must possibly be approximated).
3. Affine invariance is nice, but not always needed. Sphering can be costly in terms of precision.
4. Likewise, robustness is not always needed. There is a trade-off between robustness and computational complexity. If the data appear to be contaminated, robustified Mahalanobis depth may be employed in case of elliptically symmetric data, and spatial or halfspace depth otherwise.
5. In case of missing values, zonoid depth can be used with mean imputation.

We have covered only a few (but popular) notions of multivariate depth. Many more have been and are still proposed in the literature. To be meaningful they should be sufficiently invariant (at least orthogonal and translation invariant), reflect asymmetries of the data, and be computationally feasible for practically relevant dimensions  $d$  and data lengths  $n$ , employing either exact or sufficiently precise approximative procedures.

## References

- Agostinelli, C. and M. Romanazzi (2011). Local depth. *Journal of Statistical Planning and Inference* 141(2), 817–830.
- Azzalini, A. and A. D. Valle (1996). The multivariate skew-normal distribution. *Biometrika* 83(4), 715–726.
- Barber, C. B., D. P. Dobkin, and H. Huhdanpaa (1996). The quickhull algorithm for convex hulls. *ACM Trans. Math. Softw.* 22(4), 469–483.
- Barnett, V. (1976). The ordering of multivariate data. *Journal of the Royal Statistical Society, Series A* 139, 318–352. With discussion.
- Cascos, I. and M. López-Díaz (2016). On the uniform consistency of the zonoid depth. *Journal of Multivariate Analysis* 143, 394–397.

- Cascos, I. and I. Molchanov (2007). Multivariate risks and depth-trimmed regions. *Finance and Stochastics* 11, 373–397.
- Chen, Y., X. Dang, H. Peng, and H. L. Bart (2009). Outlier detection with the kernelized spatial depth function. *IEEE Transactions on Pattern Analysis and Machine Intelligence* 31(2), 288–305.
- Cuesta-Albertos, J. and A. Nieto-Reyes (2008a). The random Tukey depth. *Computational Statistics and Data Analysis* 52, 4979–4988.
- Cuesta-Albertos, J. and A. Nieto-Reyes (2008b). The Tukey and the random Tukey depths characterize discrete distributions. *Journal of Multivariate Analysis* 99(10), 2304–2311.
- Donoho, D. L. and M. Gasko (1992). Breakdown properties of location estimates based on halfspace depth and projected outlyingness. *Annals of Statistics* 20, 1803–1827.
- Dümbgen, L. (1992). Limit theorems for the simplicial depth. *Statistics and Probability Letters* 14, 119–128.
- Dutta, S., S. Sarkar, and A. K. Ghosh (2016). Multi-scale classification using localized spatial depth. *Journal of Machine Learning Research* 17(218), 1–30.
- Dyckerhoff, R. (2002). Datentiefe: Begriff, Berechnung, Tests. Mimeo, Fakultät für Wirtschafts-und Sozialwissenschaften, Universität zu Köln.
- Dyckerhoff, R. (2004). Data depths satisfying the projection property. *Allgemeines Statistisches Archiv* 88, 163–190.
- Dyckerhoff, R., G. Koshevoy, and K. Mosler (1996). Zonoid data depth: Theory and computation. In A. Pratt (Ed.), *COMPSTAT 1996. Proceedings in Computational Statistics*, Heidelberg, pp. 235–240. Physica-Verlag.
- Dyckerhoff, R., C. Ley, and D. Paindaveine (2015). Depth-based runs tests for bivariate central symmetry. *Annals of the Institute of Statistical Mathematics* 67(5), 917–941.
- Dyckerhoff, R. and K. Mosler (2011). Weighted-mean trimming of multivariate data. *Journal of Multivariate Analysis*, 102, 405–421.
- Dyckerhoff, R. and P. Mozharovskiy (2016). Exact computation of the halfspace depth. *Computational Statistics and Data Analysis* 98, 19–30.
- Eddy, W. F. (1981). Graphics for the multivariate two-sample problem: Comment. *Journal of the American Statistical Association* 76(374), 287–289.

- Elmore, R. T., T. P. Hettmansperger, and F. Xuan (2006). Spherical data depth and a multivariate median. *DIMACS Series in Discrete Mathematics and Theoretical Computer Science* 72, 87.
- Febrero-Bande, M. and M. de la Fuente (2012). Statistical computing in functional data analysis: The r package fda.usc. *Journal of Statistical Software, Articles* 51(4), 1–28.
- Febrero-Bande, M. and M. Oviedo de la Fuente (2012). Statistical computing in functional data analysis: The R package fda.usc. *Journal of Statistical Software* 51(4), 1–28.
- Fischer, D., K. Mosler, J. Möttönen, K. Nordhausen, O. Pokotylo, and D. Vogel (2020). Computing the oja median in r: The package ojanp. *Journal of Statistical Software, Articles* 92(8), 1–36.
- Genest, M., J. Masse, and J. Plante (2017). Depth: Nonparametric depth functions for multivariate analysis. r package version 2.1-1.1.
- Gijbels, I. and S. Nagy (2017). On a general definition of depth for functional data. *Statistical Science* 32(4), 630–639.
- Hoberg, R. (2000). Cluster analysis based on data depth. In H. Kiers, J.-P. Rasson, P. Groenen, and M. Schader (Eds.), *Data Analysis, Classification, and Related Methods*, Berlin, pp. 17–22. Springer.
- Hu, Y., Y. Wang, Y. Wu, Q. Li, and C. Hou (2011). Generalized Mahalanobis depth in the reprocing kernel hilbert space. *Statistical Papers* 52, 511–522.
- Hubert, M., P. J. Rousseeuw, and P. Segaeert (2015). Multivariate functional outlier detection. *Statistical Methods and Applications* 24, 177–202.
- Kleindessner, M. and U. Von Luxburg (2017). Lens depth function and k-relative neighborhood graph: versatile tools for ordinal data analysis. *Journal of Machine Learning Research* 18(1), 1889–1940.
- Koshevoy, G. (1997). Integrable  $L$ -statistics, depths and ranks. Unpublished mimeo.
- Koshevoy, G. (2003). Lift-zonoid and multivariate depths. In *Developments in Robust Statistics*, pp. 194–202. Springer.
- Koshevoy, G. and K. Mosler (1997). Zonoid trimming for multivariate distributions. *Annals of Statistics* 25(5), 1998–2017.
- Koshevoy, G. A. (2002). The Tukey depth characterizes the atomic measure. *Journal of Multivariate Analysis* 83(2), 360–364.



- Kosiorowski, D. and Z. Zawadzki (2014). DepthProc: An R package for robust exploration of multidimensional economic phenomena. arXiv:1408.4542.
- Lange, T., K. Mosler, and P. Mozharovskyi (2014a). DD $\alpha$ -classification of asymmetric and fat-tailed data. In M. Spiliopoulou, L. Schmidt-Thieme, and R. Janning (Eds.), *Data Analysis, Machine Learning and Knowledge Discovery*, Cham, pp. 71–78. Springer International Publishing.
- Lange, T., K. Mosler, and P. Mozharovskyi (2014b). Fast nonparametric classification based on data depth. *Statistical Papers* 55, 49–69.
- Li, J., J. Cuesta-Albertos, and R. Y. Liu (2012). dd-classifier: Nonparametric classification procedure based on dd-plot. *Journal of the American Statistical Association* 107(498), 737–753.
- Liu, R. Y. (1990). On a notion of data depth based on random simplices. *Annals of Statistics* 18, 405–414.
- Liu, R. Y. (1992). Data depth and multivariate rank tests. In Y. Dodge (Ed.), *L<sub>1</sub>-Statistics Analysis and Related Methods*, pp. 279–294. Amsterdam: North-Holland.
- Liu, R. Y., J. M. Parelius, and K. Singh (1999). Multivariate analysis by data depth: Descriptive statistics, graphics and inference. *Annals of Statistics* 27(3), 783–858. With discussion.
- Liu, X. and Y. Zuo (2014, Jan). Computing projection depth and its associated estimators. *Statistics and Computing* 24(1), 51–63.
- Liu, X. and Y. Zuo (2015). Comppd: A matlab package for computing projection depth. *Journal of Statistical Software, Articles* 65(2), 1–21.
- Liu, Z. and R. Modarres (2011). Lens data depth and median. *Journal of Nonparametric Statistics* 23(4), 1063–1074.
- Lopuhaa, H. P., P. J. Rousseeuw, et al. (1991). Breakdown points of affine equivariant estimators of multivariate location and covariance matrices. *The Annals of Statistics* 19(1), 229–248.
- Mahalanobis, P. C. (1936). On the generalized distance in statistics. *Proceedings of the National Academy of India* 12, 49–55.
- Mahalanobish, O. and S. Karmakar (2015). *depth.plot: Multivariate Analogy of Quantiles*. R Foundation for Statistical Computing. R package version 0.1.

- Mizera, I. and M. Volauß (2002). Continuity of halfspace depth contours and maximum depth estimators: diagnostics of depth-related methods. *Journal of Multivariate Analysis* 83(2), 365–388.
- Mosler, K. (2002). *Multivariate Dispersion, Central Regions and Depth: The Lift Zonoid Approach*. New York: Springer.
- Mosler, K. and P. Bazovkin (2014). Stochastic linear programming with a distortion risk constraint. *OR Spectrum* 36(4), 949–969.
- Mosler, K. and Y. Polyakova (2012). General notions of depth for functional data. arXiv:1208.1981.
- Mozharovskiy, P., K. Mosler, and T. Lange (2015). Classifying real-world data with the  $DD\alpha$ -procedure. *Advances in Data Analysis and Classification* 9(3), 287–314.
- Nagy, S. (2017). Monotonicity properties of spatial depth. *Statistics & Probability Letters* 129, 373–378.
- Nagy, S. (2019). Halfspace depth does not characterize probability distributions. *Statistical Papers*. in print.
- Nagy, S., R. Dyckerhoff, and P. Mozharovskiy (2019). Uniform convergence rates for the approximated halfspace and projection depth. arXiv:1910.05956.
- Nagy, S., I. Gijbels, M. Omelka, and D. Hlubinka (2016). Integrated depth for functional data: Statistical properties and consistency. *ESAIM: Probability and Statistics* 20, 95–130.
- Nagy, S., C. Schütt, E. M. Werner, et al. (2019). Halfspace depth and floating body. *Statistics Surveys* 13, 52–118.
- Niinimaa, A. and H. Oja (1995). On the influence functions of certain bivariate medians. *Journal of the Royal Statistical Society, Series B* 57, 565–574.
- Niinimaa, A., H. Oja, and M. Tableman (1990). The finite-sample breakdown point of the Oja bivariate median and of the corresponding half-samples version. *Statistics and Probability Letters* 10, 325–328.
- Nordhausen, K. and D. E. Tyler (2015). A cautionary note on robust covariance plug-in methods. *Biometrika* 102(3), 573–588.
- Oja, H. (1983). Descriptive statistics for multivariate distributions. *Statistics and Probability Letters* 1, 327–332.

- Paindaveine, D. and G. Van Bever (2013). From depth to local depth: a focus on centrality. *Journal of the American Statistical Association* 108(503), 1105–1119.
- Pokotylo, O. and K. Mosler (2019). Classification with the pot–pot plot. *Statistical Papers* 60(3), 553–581.
- Pokotylo, O., P. Mozharovskyi, and R. Dyckerhoff (2019). Depth and depth-based classification with r package ddalpha. *Journal of Statistical Software, Articles* 91(5), 1–46.
- Pokotylo, O., P. Mozharovskyi, R. Dyckerhoff, and S. Nagy (2020). *ddalpha: Depth-Based Classification and Calculation of Data Depth*. R Foundation for Statistical Computing. R package version 1.3.11.
- Romanazzi, M. (2001). Influence function of halfspace depth. *Journal of Multivariate Analysis* 77, 138–161.
- Rousseeuw, P. J. and A. M. Leroy (1987). *Robust Regression and Outlier Detection*. New York: John Wiley & Sons.
- Rousseeuw, P. J. and A. Struyf (1998). Computing location depth and regression depth in higher dimensions. *Statistics and Computing* 8, 193–203.
- Segaert, P., M. Hubert, P. Rousseeuw, J. Raymaekers, and K. Vakili (2019). *mrfDepth: Depth Measures in Multivariate, Regression and Functional Settings*. R Foundation for Statistical Computing. R package version 1.0.11.
- Serfling, R. (2002). A depth function and a scale curve based on spatial quantiles. In Y. Dodge (Ed.), *Statistical Data Analysis Based on the  $L_1$ -Norm and Related Methods*, pp. 25–38. Basel: Birkhäuser.
- Tukey, J. W. (1975). Mathematics and the picturing of data. In R. James (Ed.), *Proceedings of the International Congress of Mathematicians*, Volume 2, pp. 523–531. Canadian Mathematical Congress.
- Yang, M. and R. Modarres (2018).  $\beta$ -skeleton depth functions and medians. *Communications in Statistics – Theory and Methods* 47(20), 5127–5143.
- Zawadzki, Z., D. Kosiorowski, K. Slomczynski, M. Bocian, and A. Wegrzynkiewicz (2020). *DepthProc: Statistical Depth Functions for Multivariate Analysis*. R Foundation for Statistical Computing. R package version 2.1.3.
- Zuo, Y. (2004). Robustness of weighted  $L_p$ -depth and  $L_p$ -median. *Allgemeines Statistisches Archiv* 88(2), 215–234.

- Zuo, Y. (2006). Multidimensional trimming based on projection depth. *Annals of Statistics* 34, 2211–2251.
- Zuo, Y. et al. (2003). Projection-based depth functions and associated medians. *Annals of Statistics* 31(5), 1460–1490.
- Zuo, Y. and R. Serfling (2000). General notions of statistical depth function. *Annals of Statistics* 28, 461–482.

# Supplementary Material to

## “Choosing among notions of multivariate depth statistics”

Karl Mosler

Institute of Econometrics and Statistics, University of Cologne

Pavlo Mozharovskyi

LTCI, Télécom Paris, Institut Polytechnique de Paris

### Abstract

This Supplementary Material presents detailed results of the simulation study on classification with different depths in Section 4.3 of the paper. Further, results on the approximation error of the random Tukey depth (Section 5.2) are given, as well as illustrations of the properties of local depths (Section 6.1).

## 1 A study of different depths in classification

To study depth performance in different settings, the  $DD\alpha$ -classifier (Lange et al., 2014b) is applied to classification problems in dimensions two and three.

Consider a random vector,  $Z$ , from one of the following distributions: standard normal distribution; spherical Student  $t$ -distribution with five degrees of freedom; spherical Cauchy distribution; uniform distribution on square resp. cube; skewed-normal distribution with skewness parameter equal to five in the first coordinate according to Azzalini and Valle (1996); product of independent univariate exponential distributions having parameter 1.

First, location alternatives are constructed. The two classes correspond to  $X_1 \stackrel{d}{=} \boldsymbol{\mu}_1 + Z$  and  $X_2 \stackrel{d}{=} \boldsymbol{\mu}_2 + Z$ , where  $\boldsymbol{\mu}_1 = (0, 0)^\top$ ,  $\boldsymbol{\mu}_2 = (1, 0)^\top$  in dimension  $d = 2$  and  $\boldsymbol{\mu}_1 = (0, 0, 0)^\top$ ,  $\boldsymbol{\mu}_2 = (1, 0, 0)^\top$  in dimension  $d = 3$ . Training and test samples include twice 100 and twice 500 observations, respectively. Figure 1 shows samples from the two classes, for each of the six classification problems in dimension two.

The  $DD\alpha$ -classifier is obtained in two steps: First each training point is represented by its depth values regarding the two training classes, which results in a two-dimensional

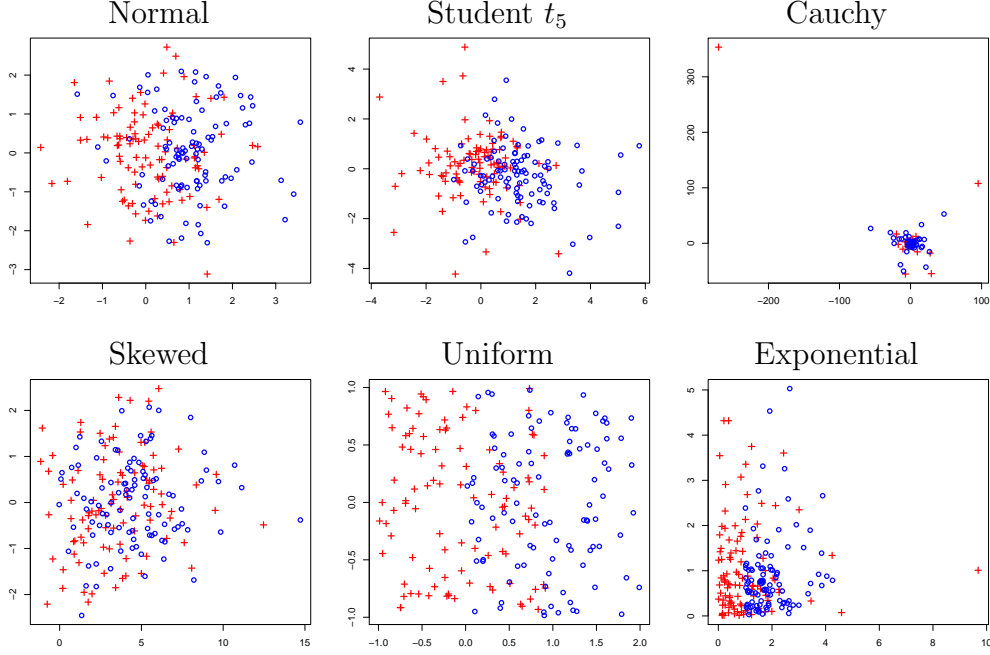


Figure 1: Samples of six location alternatives,  $d = 2$ .

*DD-plot*. Then, by the  $\alpha$ -procedure, a rule is determined that separates the training points in the *DD*-plot. New items are similarly represented and then classified by the *DD* $\alpha$ -rule. For details, see Lange et al. (2014b).

Figure 2 shows boxplots of the error rates on the two-dimensional classification problems over 100 runs while Table 1 indicates medians and median absolute deviations from the medians over 100 runs as well. These error rates are also contrasted with those of the optimal Bayes rule, which assigns a new point to the class of higher population density. The same is done in Figure 3 and Table 2 for the three-dimensional problems.

The projection depth is approximated by using 1000 directions, all other depths are exactly computed.

Obviously, a point that has depth 0 regarding both classes, a so called *outsider* (Lange et al., 2014b), cannot be classified by the *DD* $\alpha$ -rule. In our study we neglect outsiders and measure the classification error on the remaining points only. Note that the halfspace, simplicial, zonoid and onion depths vanish outside the convex hull of the data. For a fair comparison, the classification error for all the depths is measured only for points located inside the convex hull of at least one of the training samples.

A first look at Figure 2 reveals that for our location alternatives in dimension two the best depth-based error rate is generally not far from the optimal Bayes rate, both medians being marked by (solid and dashed, respectively) horizontal lines. More precisely, the

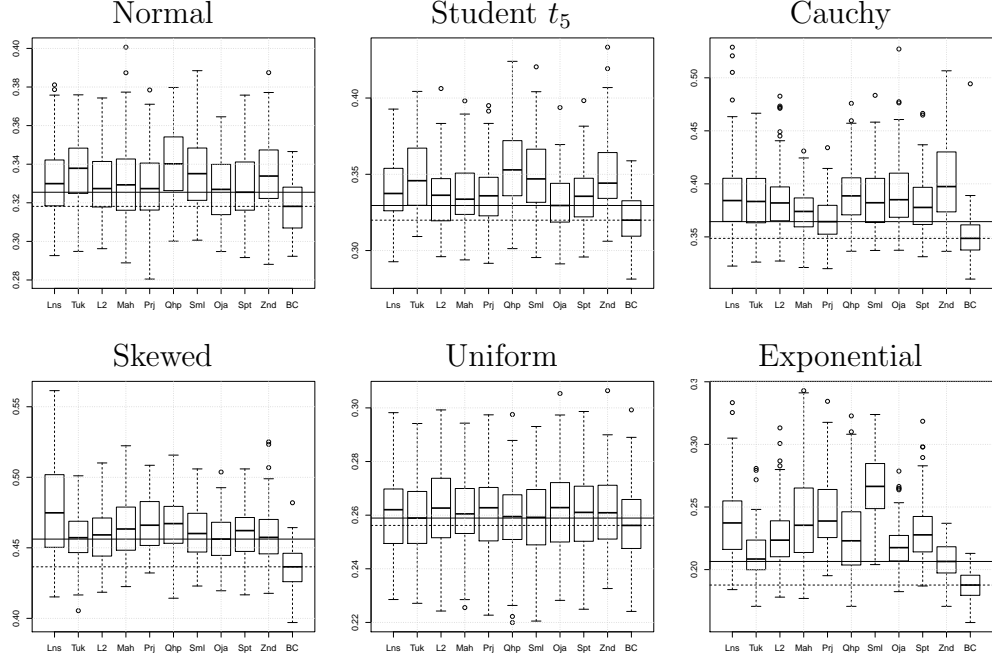


Figure 2: Boxplots of the error rates over 100 runs for the six location alternatives;  $d = 2$ .

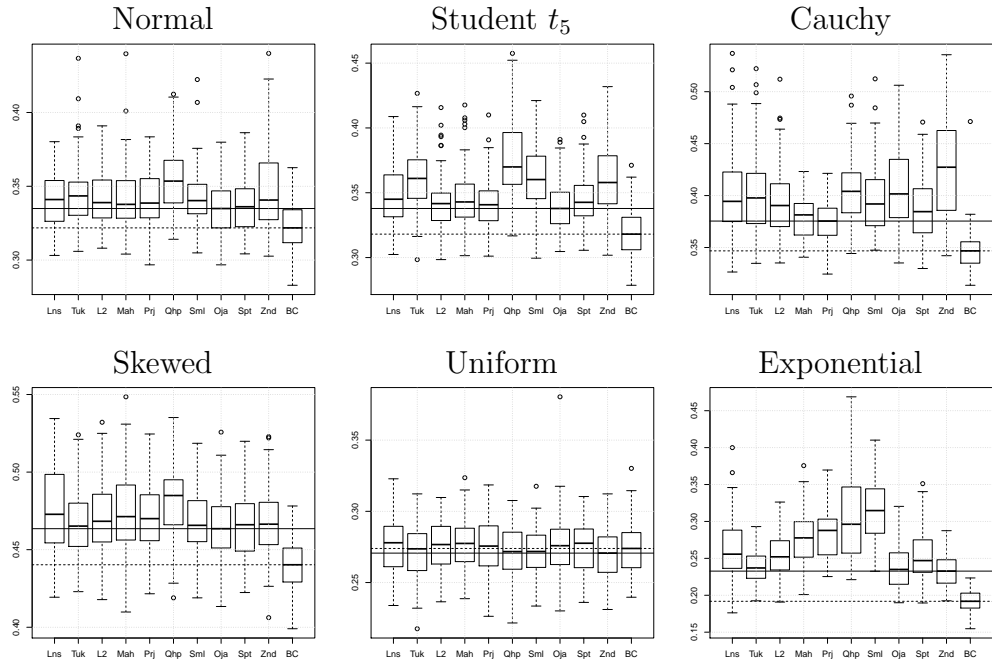


Figure 3: Boxplots of the error rates over 100 runs for the six location alternatives;  $d = 3$ .

| Depth | Norm                   | Stud                   | Cchy                   | Skwd                   | Unif                   | Expn                   |
|-------|------------------------|------------------------|------------------------|------------------------|------------------------|------------------------|
| Lens  | <b>0.33</b><br>(0.018) | 0.34<br>(0.021)        | 0.38<br>(0.03)         | 0.47<br>(0.038)        | <b>0.26</b><br>(0.015) | 0.24<br>(0.028)        |
| H     | 0.34<br>(0.018)        | 0.35<br>(0.027)        | 0.38<br>(0.03)         | <b>0.46</b><br>(0.016) | <b>0.26</b><br>(0.014) | <b>0.21</b><br>(0.016) |
| $L_2$ | <b>0.33</b><br>(0.017) | 0.34<br>(0.02)         | 0.38<br>(0.023)        | <b>0.46</b><br>(0.021) | <b>0.26</b><br>(0.016) | 0.22<br>(0.02)         |
| Mah   | <b>0.33</b><br>(0.02)  | <b>0.33</b><br>(0.024) | 0.37<br>(0.02)         | <b>0.46</b><br>(0.023) | <b>0.26</b><br>(0.013) | 0.24<br>(0.036)        |
| Proj  | <b>0.33</b><br>(0.017) | 0.34<br>(0.019)        | <b>0.36</b><br>(0.019) | 0.47<br>(0.023)        | <b>0.26</b><br>(0.013) | 0.24<br>(0.023)        |
| CHP   | 0.34<br>(0.021)        | 0.35<br>(0.025)        | 0.39<br>(0.026)        | 0.47<br>(0.018)        | <b>0.26</b><br>(0.012) | 0.22<br>(0.029)        |
| Sim   | 0.34<br>(0.02)         | 0.35<br>(0.026)        | 0.38<br>(0.03)         | <b>0.46</b><br>(0.019) | <b>0.26</b><br>(0.015) | 0.27<br>(0.027)        |
| Oja   | <b>0.33</b><br>(0.019) | <b>0.33</b><br>(0.018) | 0.39<br>(0.032)        | <b>0.46</b><br>(0.017) | <b>0.26</b><br>(0.016) | 0.22<br>(0.015)        |
| Spa   | <b>0.33</b><br>(0.015) | 0.34<br>(0.02)         | 0.38<br>(0.026)        | <b>0.46</b><br>(0.02)  | <b>0.26</b><br>(0.015) | 0.23<br>(0.021)        |
| Zon   | <b>0.33</b><br>(0.018) | 0.34<br>(0.021)        | 0.40<br>(0.039)        | <b>0.46</b><br>(0.017) | <b>0.26</b><br>(0.015) | <b>0.21</b><br>(0.016) |
| Bayes | 0.32<br>(0.015)        | 0.32<br>(0.016)        | 0.35<br>(0.017)        | 0.44<br>(0.015)        | 0.26<br>(0.014)        | 0.19<br>(0.012)        |

Table 1: Medians and median absolute deviations from the medians of error rates over 100 runs for the six location alternatives for different depth notions,  $d = 2$ . For each alternative, best performing depths are indicated in bold.

differences in median range from 0 for uniform data to three percent for Cauchy data; see Table 1. Things look only slightly worse in dimension three (Figure 3 and Table 2): Here differences between those medians vary from null in the uniform case to four per cent in the exponential case. Note that the first three alternatives (normal,  $t_5$ , Cauchy) consist of unimodal elliptical distributions differing in location. For those alternatives follows from Theorem 2 in Lange et al. (2014b) that the error rate of the  $DD\alpha$ -classifier converges to the optimal Bayes rate when the size of the training classes goes to infinity. The same follows for the uniform alternative from Theorem 1 in Lange et al. (2014b). For the other two alternatives (skewed normal, exponential) we have no such theoretical results.

Further, our results demonstrate that there exists no uniformly best choice of the depth notion. On uniformly distributed data all depths perform equally well. With other data



| Depth | Norm                   | Stud                   | Cchy                   | Skwd                   | Unif                   | Expn                   |
|-------|------------------------|------------------------|------------------------|------------------------|------------------------|------------------------|
| Lens  | 0.34<br>(0.021)        | 0.35<br>(0.024)        | 0.39<br>(0.034)        | 0.47<br>(0.032)        | 0.28<br>(0.02)         | 0.26<br>(0.034)        |
| H     | 0.34<br>(0.018)        | 0.36<br>(0.023)        | 0.40<br>(0.036)        | 0.47<br>(0.021)        | <b>0.27</b><br>(0.017) | 0.24<br>(0.022)        |
| $L_2$ | 0.34<br>(0.018)        | <b>0.34</b><br>(0.017) | 0.39<br>(0.03)         | 0.47<br>(0.023)        | 0.28<br>(0.019)        | 0.25<br>(0.027)        |
| Mah   | 0.34<br>(0.019)        | <b>0.34</b><br>(0.019) | <b>0.38</b><br>(0.022) | 0.47<br>(0.026)        | 0.28<br>(0.018)        | 0.28<br>(0.035)        |
| Proj  | 0.34<br>(0.018)        | <b>0.34</b><br>(0.018) | <b>0.38</b><br>(0.02)  | 0.47<br>(0.022)        | 0.28<br>(0.021)        | 0.29<br>(0.034)        |
| CHP   | 0.35<br>(0.022)        | 0.37<br>(0.025)        | 0.40<br>(0.028)        | 0.48<br>(0.02)         | <b>0.27</b><br>(0.019) | 0.30<br>(0.063)        |
| Sim   | 0.34<br>(0.014)        | 0.36<br>(0.023)        | 0.39<br>(0.033)        | 0.47<br>(0.02)         | <b>0.27</b><br>(0.017) | 0.31<br>(0.044)        |
| Oja   | <b>0.33</b><br>(0.019) | <b>0.34</b><br>(0.018) | 0.40<br>(0.042)        | <b>0.46</b><br>(0.019) | 0.28<br>(0.018)        | <b>0.23</b><br>(0.031) |
| Spa   | 0.34<br>(0.018)        | <b>0.34</b><br>(0.017) | <b>0.38</b><br>(0.03)  | 0.47<br>(0.024)        | 0.28<br>(0.019)        | 0.25<br>(0.027)        |
| Zon   | 0.34<br>(0.025)        | 0.36<br>(0.028)        | 0.43<br>(0.058)        | 0.47<br>(0.02)         | <b>0.27</b><br>(0.018) | <b>0.23</b><br>(0.023) |
| Bayes | 0.32<br>(0.017)        | 0.32<br>(0.019)        | 0.35<br>(0.015)        | 0.44<br>(0.016)        | 0.27<br>(0.018)        | 0.19<br>(0.014)        |

Table 2: Medians and median absolute deviations from the medians of classification error rates over 100 runs for the six location alternatives for different depth notions;  $d = 3$ . Best performing depth notions for each alternative are indicated in bold.

slight differences prevail. When the data are elliptically symmetric (normal, Student, and Cauchy cases) onion depth, simplicial depth and Tukey depth appear to be less recommendable, similarly zonoid depth, when the data are prone to outliers (Cauchy case). Asymmetric data (as in the skewed and exponential cases) are worse classified with simplicial, lens, projection and Mahalanobis depth. Consequently, for the considered location alternatives, three depths show an overall acceptable behavior, *viz.* the Oja, spatial, and  $\mathbb{L}_2$  depths.

Next we study the classification of data that differ additionally in scale. Based on the above location alternatives, six location-scale alternatives are generated by multiplying the last coordinate of the second class with 2. The simplicity of this setting is explained by the affine invariance of all depths considered. Figure 4 shows six samples of the training

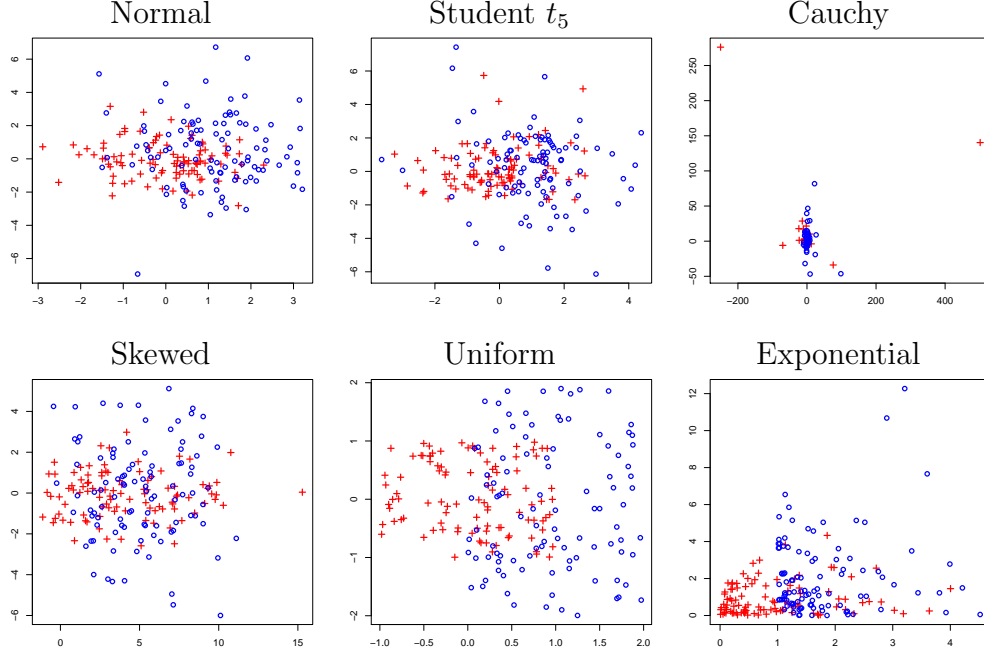


Figure 4: Examples of the six location-scale alternatives,  $d = 2$ .

classes in dimension two. The parameters of the simulation and the  $DD\alpha$ -procedure are the same as above.

Similarly, Figures 5 and 6 together with Tables 3 and 4 exhibit the obtained error rates and their medians from classifying the location-scale alternatives.

It comes out that the depth-based classification of location-scale alternatives, like that of pure location alternatives, yields median error rates that come close to the optimal Bayes rates. This means, with the best choice of depth we get error rates that usually differ just by one or two percent from the Bayes rate, and by at most four percent.

Again, there exists no uniformly best depth. The boxplots in Figures 5 and 6 give an idea of the appropriateness of different notions. When the location-scale alternatives include elliptically symmetric distributions, Tukey, onion, simplicial and zonoid depth seem to perform worse than others. With asymmetric data also simplicial and Mahalanobis depth operate more poorly. So, for this sort of location-scale alternatives, the remaining depths, *viz.* the lens, Oja, the spatial and the  $\mathbb{L}_2$  depth show an overall satisfactory behavior.

To further investigate an eventual convergence to the optimal Bayes rate, we increase the number of observations. Training observations total from 200 up to 20000, and five times more observations than trained are tested. Figure 7 exhibits, for each of the two-dimensional settings considered above, the difference (on an average, over 100 runs) between the observed error rate and the Bayes rate. We restrict the presentation to the halfspace

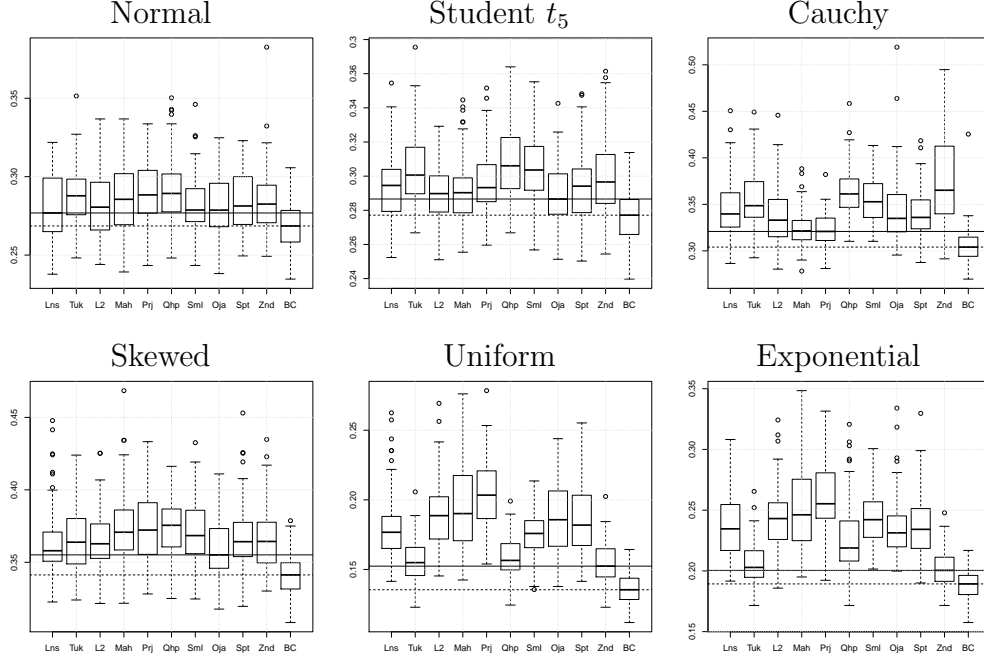


Figure 5: Boxplots of the error rates over 100 runs for the six location-scale alternatives;  $d = 2$ .

depth.

One observes that in all cases the  $DD\alpha$  error rate decreases and approaches the Bayes rate when the number of observations increases. (An exception is the uniform location alternative, where the error rate always comes close to the Bayes rate.) While convergence for the first four location alternatives follows from theory, it is new for the remaining eight ones. Note that, in our implementation, the  $DD\alpha$ -classifier for separating the  $DD$ -plot employs polynomials whose degree is bounded by three. Li et al. (2012) provide further theoretical results and examples how classification in the  $DD$ -plot can produce error rates that come close to the base rate. This gives hope that depth-based classifiers can be of use in a rather wide range of applications, also beyond elliptically symmetric distributions.

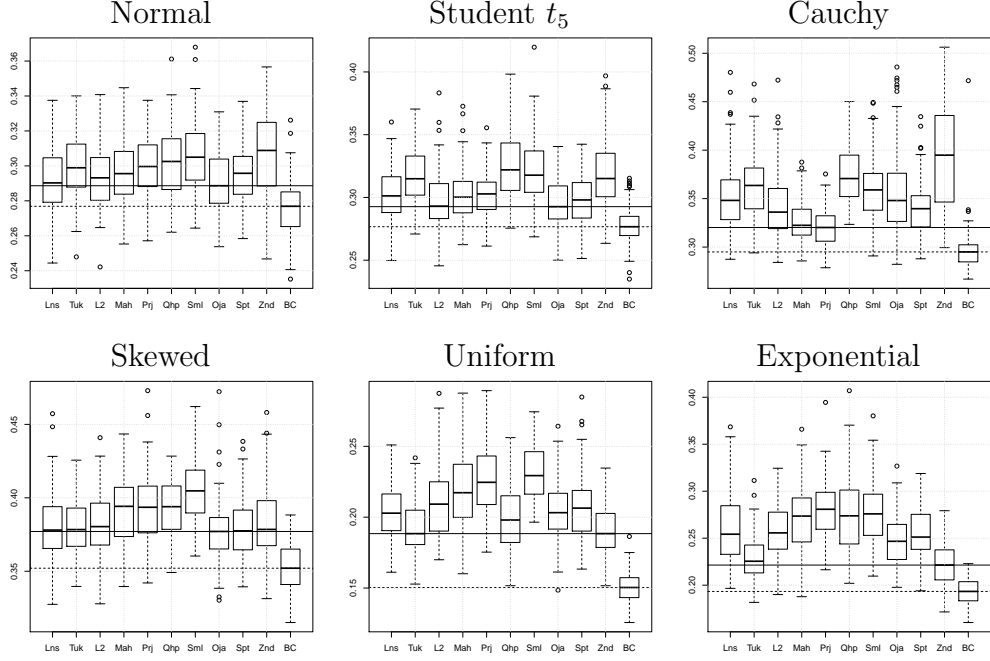


Figure 6: Boxplots of the error rates over 100 runs for the six location-scale alternatives;  $d = 3$ .

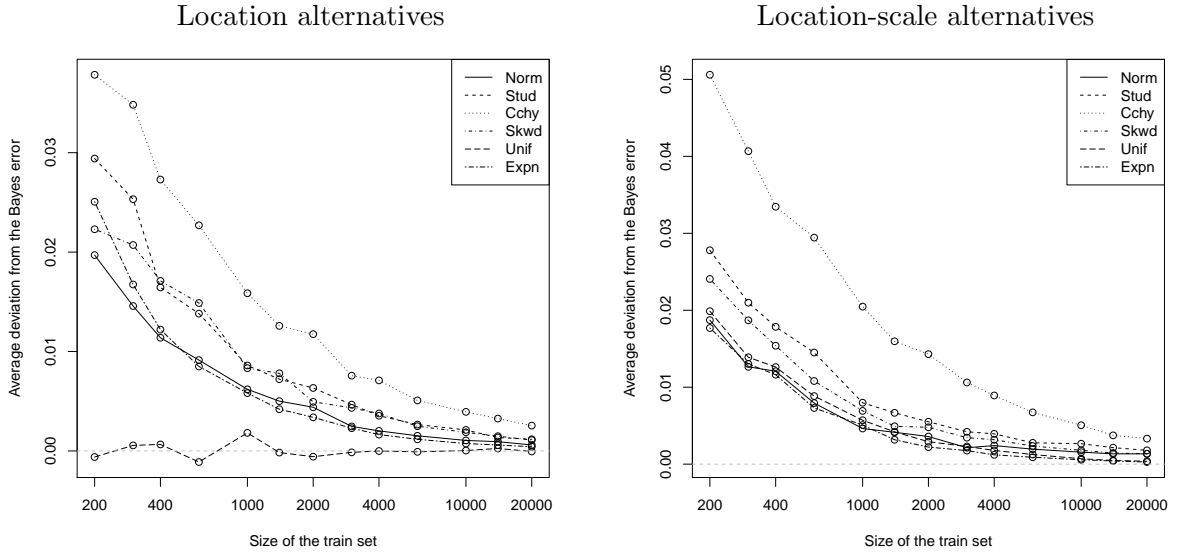


Figure 7: Average difference between the error rate of the  $DD\alpha$ -classifier (using halfspace depth) and the optimal Bayes rate when observations are increased; location alternatives (left), location-scale alternatives (right).

| Depth | Norm                   | Stud                   | Cchy                   | Skwd                   | Unif                   | Expn                   |
|-------|------------------------|------------------------|------------------------|------------------------|------------------------|------------------------|
| Lens  | <b>0.28</b><br>(0.022) | <b>0.29</b><br>(0.017) | 0.34<br>(0.022)        | <b>0.36</b><br>(0.015) | 0.18<br>(0.017)        | 0.23<br>(0.029)        |
| H     | 0.29<br>(0.017)        | 0.30<br>(0.021)        | 0.35<br>(0.031)        | <b>0.36</b><br>(0.023) | <b>0.15</b><br>(0.015) | <b>0.20</b><br>(0.014) |
| $L_2$ | <b>0.28</b><br>(0.022) | <b>0.29</b><br>(0.016) | 0.33<br>(0.028)        | <b>0.36</b><br>(0.018) | 0.19<br>(0.022)        | 0.24<br>(0.022)        |
| Mah   | 0.29<br>(0.024)        | <b>0.29</b><br>(0.016) | <b>0.32</b><br>(0.015) | 0.37<br>(0.02)         | 0.19<br>(0.033)        | 0.25<br>(0.037)        |
| Proj  | 0.29<br>(0.018)        | <b>0.29</b><br>(0.013) | <b>0.32</b><br>(0.018) | 0.37<br>(0.026)        | 0.20<br>(0.025)        | 0.26<br>(0.023)        |
| CHP   | 0.29<br>(0.018)        | 0.31<br>(0.02)         | 0.36<br>(0.022)        | 0.38<br>(0.02)         | 0.16<br>(0.013)        | 0.22<br>(0.023)        |
| Sim   | <b>0.28</b><br>(0.018) | 0.30<br>(0.019)        | 0.35<br>(0.026)        | 0.37<br>(0.021)        | 0.18<br>(0.015)        | 0.24<br>(0.022)        |
| Oja   | <b>0.28</b><br>(0.018) | <b>0.29</b><br>(0.016) | 0.33<br>(0.03)         | <b>0.36</b><br>(0.019) | 0.19<br>(0.029)        | 0.23<br>(0.02)         |
| Spa   | <b>0.28</b><br>(0.023) | <b>0.29</b><br>(0.02)  | 0.34<br>(0.022)        | <b>0.36</b><br>(0.017) | 0.18<br>(0.025)        | 0.23<br>(0.024)        |
| Zon   | <b>0.28</b><br>(0.018) | 0.30<br>(0.02)         | 0.37<br>(0.046)        | <b>0.36</b><br>(0.021) | <b>0.15</b><br>(0.013) | <b>0.20</b><br>(0.014) |
| Bayes | 0.27<br>(0.015)        | 0.28<br>(0.014)        | 0.30<br>(0.015)        | 0.34<br>(0.013)        | 0.14<br>(0.011)        | 0.19<br>(0.011)        |

Table 3: Medians and median absolute deviations from the medians of classification error rates over 100 runs for the six location-scale alternatives for different depth notions;  $d = 2$ . Best performing depth notions for each alternative are indicated in bold.

| Depth | Norm                   | Stud                   | Cchy                   | Skwd                   | Unif                   | Expn                   |
|-------|------------------------|------------------------|------------------------|------------------------|------------------------|------------------------|
| Lens  | <b>0.29</b><br>(0.017) | 0.30<br>(0.021)        | 0.35<br>(0.03)         | <b>0.38</b><br>(0.023) | 0.20<br>(0.019)        | 0.25<br>(0.036)        |
| H     | 0.3<br>(0.018)         | 0.31<br>(0.026)        | 0.36<br>(0.031)        | <b>0.38</b><br>(0.019) | <b>0.19</b><br>(0.019) | 0.23<br>(0.022)        |
| $L_2$ | <b>0.29</b><br>(0.018) | <b>0.29</b><br>(0.017) | 0.34<br>(0.029)        | <b>0.38</b><br>(0.021) | 0.21<br>(0.026)        | 0.26<br>(0.029)        |
| Mah   | 0.30<br>(0.018)        | 0.30<br>(0.019)        | <b>0.32</b><br>(0.018) | 0.39<br>(0.023)        | 0.22<br>(0.026)        | 0.27<br>(0.033)        |
| Proj  | 0.30<br>(0.018)        | 0.30<br>(0.017)        | <b>0.32</b><br>(0.02)  | 0.39<br>(0.022)        | 0.22<br>(0.026)        | 0.28<br>(0.03)         |
| CHP   | 0.30<br>(0.022)        | 0.32<br>(0.026)        | 0.37<br>(0.031)        | 0.39<br>(0.021)        | 0.20<br>(0.025)        | 0.27<br>(0.042)        |
| Sim   | 0.30<br>(0.02)         | 0.32<br>(0.025)        | 0.36<br>(0.03)         | 0.40<br>(0.022)        | 0.23<br>(0.022)        | 0.28<br>(0.033)        |
| Oja   | <b>0.29</b><br>(0.018) | <b>0.29</b><br>(0.019) | 0.35<br>(0.037)        | <b>0.38</b><br>(0.015) | 0.20<br>(0.019)        | 0.25<br>(0.028)        |
| Spa   | 0.30<br>(0.015)        | 0.30<br>(0.021)        | 0.34<br>(0.025)        | <b>0.38</b><br>(0.02)  | 0.21<br>(0.022)        | 0.25<br>(0.032)        |
| Zon   | 0.31<br>(0.025)        | 0.32<br>(0.025)        | 0.39<br>(0.066)        | <b>0.38</b><br>(0.022) | <b>0.19</b><br>(0.017) | <b>0.22</b><br>(0.024) |
| Bayes | 0.28<br>(0.016)        | 0.28<br>(0.012)        | 0.30<br>(0.013)        | 0.35<br>(0.019)        | 0.15<br>(0.011)        | 0.19<br>(0.015)        |

Table 4: Medians and median absolute deviations from the medians of classification error rates over 100 runs for the six location-scale alternatives for different depth notions;  $d = 3$ . Best performing depth notions for each alternative are indicated in bold.

## 2 Approximation errors of random Tukey depth

The halfspace (= Tukey) depth  $D^H$  satisfies the projection property,

$$D^H(\mathbf{y}|P) = \inf_{\mathbf{p} \in S^{d-1}} D^H(\langle \mathbf{p}, \mathbf{y} \rangle | P_{\mathbf{p}}), \quad \mathbf{y} \in \mathbb{R}^d, \quad (30)$$

where  $\mathbf{X} \sim P$  and  $P_{\mathbf{p}}$  is the distribution of the random variable  $\langle \mathbf{p}, \mathbf{X} \rangle$ , that is, of  $\mathbf{X}$  projected on a ray from 0 in direction  $\mathbf{p}$ . Thus, an upper bound of the depth is obtained by using a finite set  $S \subset S^{d-1}$  of directions and taking the minimum,

$$D^{RTD}(\mathbf{y}|P) = \min_{\mathbf{p} \in S} D(\langle \mathbf{p}, \mathbf{y} \rangle | P_{\mathbf{p}}). \quad (31)$$

With  $S$  randomly chosen,  $D^{RTD}$  is known as the *random Tukey depth*; see Cuesta-Albertos and Nieto-Reyes (2008a) and Section 5.2 of the paper. Of interest is the *relative error* incurred by this approximation,

$$\frac{D^{RTD}(\mathbf{y}|P) - D^H(\mathbf{y}|P)}{D^H(\mathbf{y}|P)},$$

as well as the *absolute error*,

$$D^{RTD}(\mathbf{y}|P) - D^H(\mathbf{y}|P).$$

Figures 8 and 9 exhibit boxplots of relative and absolute errors of the random Tukey depth, when a set  $S$  of 1000 directions is employed. Further, Figure 10 indicates the portion of observations for which the depth can be exactly calculated.

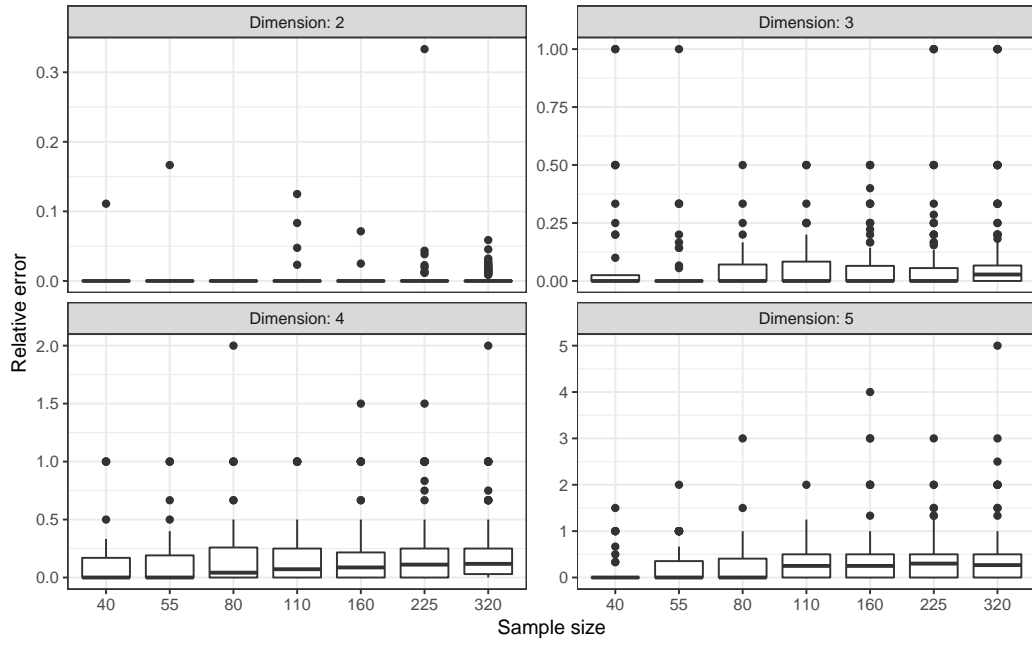


Figure 8: Relative error of the random Tukey depth when approximating at 1000 directions.

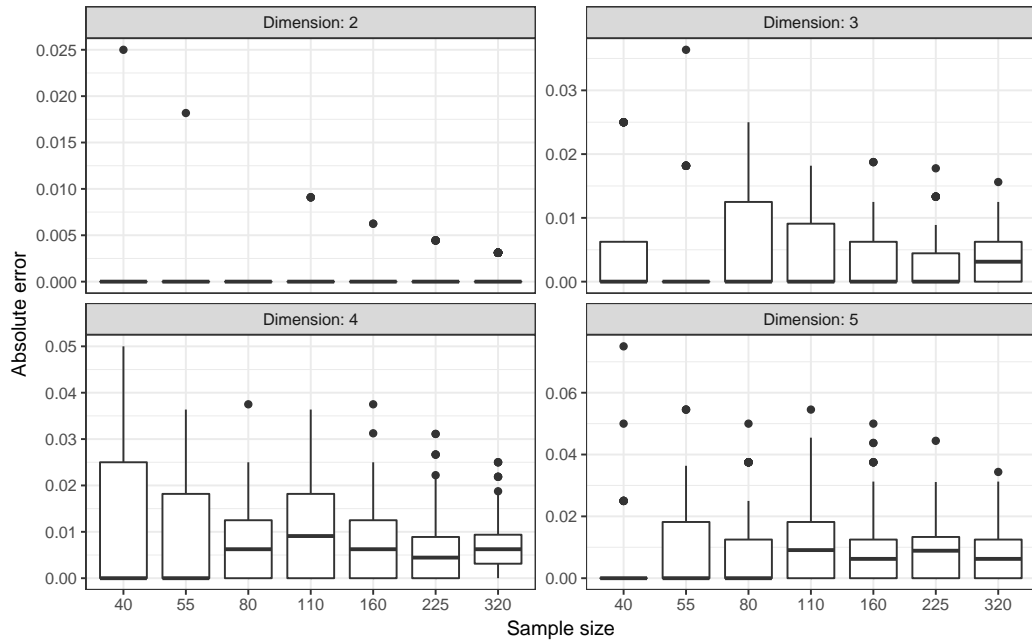


Figure 9: Absolute error of the random Tukey depth when approximating at 1000 directions.



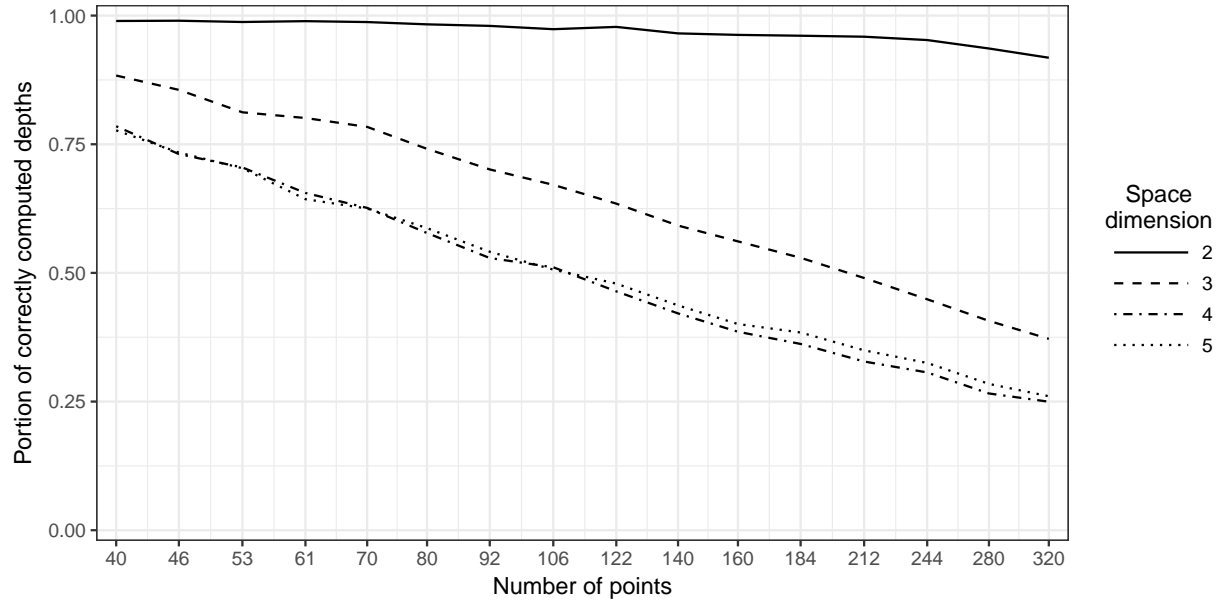


Figure 10: Average rates of achieving the exact value of Tukey depth when calculating the random Tukey depth at 1000 directions. The directions are uniformly distributed on the unit sphere, and the average is taken over all points of a standard normal sample with respect to the remaining sample, given  $d$  and  $n$ .

### 3 On local depths

Figure 11 exhibits regions of the localized Mahalanobis, zonoid and halfspace depths using the localization approach of Paindaveine and Van Bever (2013). The three samples contain 300 observations from a moon-shaped, a bimodal, and a trimodal distribution, respectively. The localization parameter is 0.33. As we see, localization is able to improve the fit of a multimodal distribution. On the other hand, spurious high-depth zones can arise (here, one for the bimodal and four for the trimodal data), due to the centrality-proneness of depth. In applications the localization parameter has to be properly chosen, depending on the data and the problem at hand. This requires prior information or (e.g. in supervised classification) tuning.

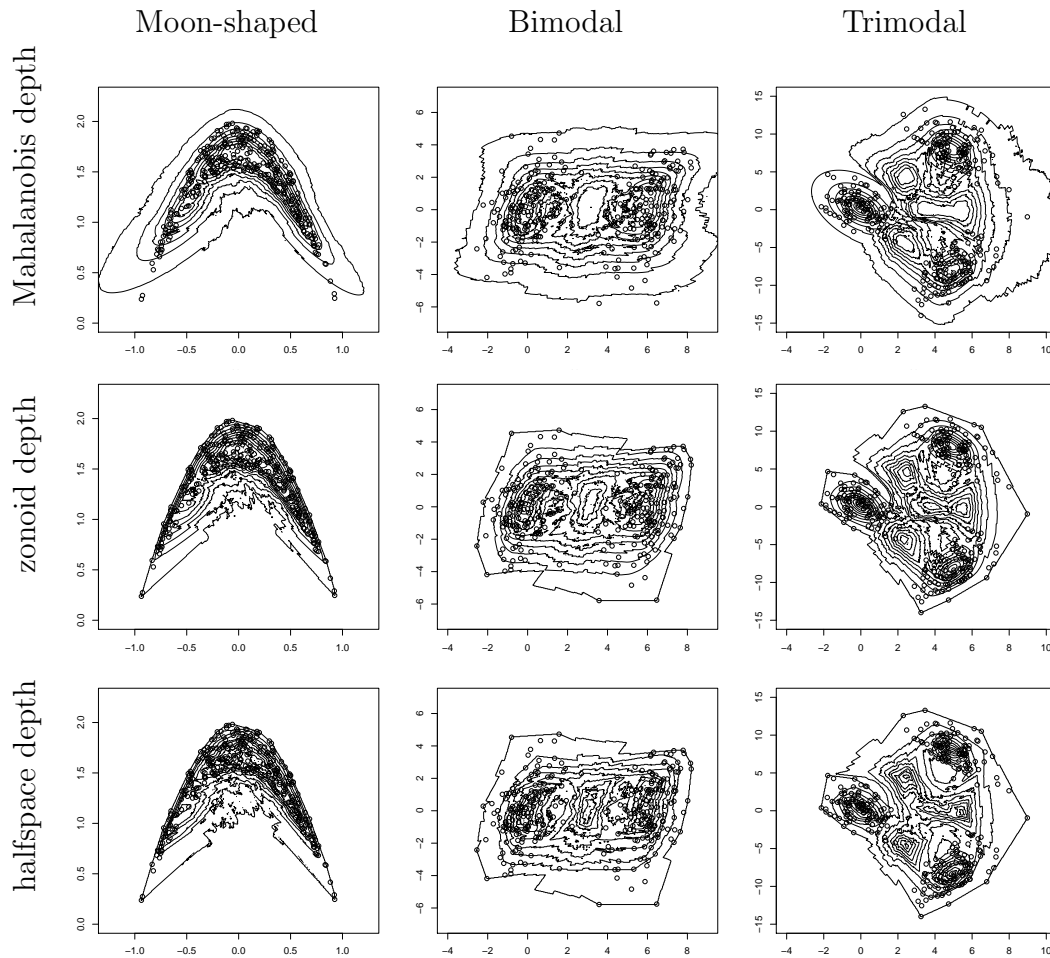


Figure 11: Depth regions for 300 points from moon-shaped (left), bimodal (middle), and trimodal (right) using localized (Paindaveine and Van Bever, 2013) Mahalanobis (top), zonoid (middle), and halfspace (bottom) depths for the localization parameter 0.33.